Title: Chronic high-sugar diet in adulthood protects *Caenorhabditis elegans* from 6-OHDA induced dopaminergic neurodegeneration

Authors and Affiliation: Katherine S. Morton[1], Jessica H. Hartman[1,2], Nathan Heffernan[1], Ian T. Ryde[1], Isabel W. Kenny-Ganzert [3], Lingfeng Meng[1], David R. Sherwood[3], Joel N. Meyer[1]

[1]Nicholas School of Environment, Duke University

[2]Biochemistry and Molecular Biology, Medical University of South Carolina

[3]Department of Biology, Duke University

Declarations: The authors declare no competing interests

Abstract

Background: Diets high in saturated fat and sugar, termed 'western diets', have been associated with several negative health outcomes, including increased risk for neurodegenerative disease. Parkinson's Disease (PD) is the second most prevalent neurodegenerative disease and is characterized by the progressive death of dopaminergic neurons in the brain. We build upon previous work characterizing the impact of high sugar diets in *Caenorhabditis elegans* to mechanistically evaluate the relationship between high sugar diets and dopaminergic neurodegeneration.

Results: Adult high glucose and fructose diets, or exposure from day 1-5 of adulthood, led to increased lipid content and shorter lifespan and decreased reproduction. However, in contrast to previous reports, we found that adult chronic high-glucose and high-fructose diets did not induce dopaminergic neurodegeneration alone and were protective from 6-hydroxydopamine (6-OHDA) induced degeneration. Neither sugar altered baseline electron transport chain function, and both increased vulnerability to organism-wide ATP depletion when the electron transport chain was inhibited, arguing against energetic rescue as a basis for neuroprotection. The induction of oxidative stress by 6-OHDA is hypothesized to contribute to its pathology, and high sugar diets prevented this increase in the soma of the dopaminergic neurons. However, we did not find increased expression of antioxidant enzymes or glutathione levels. Instead, we found evidence suggesting downregulation of the dopamine reuptake transporter *dat-1* that could result in decreased 6-OHDA uptake.

Conclusion: Our work uncovers a neuroprotective role for high sugar diets, despite concomitant decreases in lifespan and reproduction. Our results support the broader finding that ATP depletion alone is insufficient to induce dopaminergic neurodegeneration, whereas increased neuronal oxidative stress may drive degeneration. Finally, our work highlights the importance of evaluating lifestyle by toxicant interactions.

Keywords:

Glucose, Fructose, Neurodegeneration, Oxidative Stress, C. elegans

65 Background:

66 In 2019 the average American consumed 50.0 g (190 calories) of refined cane or beet sugar and
67 29.3 g (111 calories) of high-fructose corn syrup per day in addition to other added caloric sweeteners
68 and naturally occurring sugars (1). Despite a small 0.71% decrease in caloric sweetener consumption
69 since 2016, this still often exceeds the World Health Organization recommendation of less than 10% of
70 total caloric intake (2). Glucose and fructose are the most consumed sugars, as the majority of sugar
71 intake in the United States comprises refined cane or beet sugar, high-fructose corn syrup, and foods
72 naturally containing glucose and fructose (3). Referred to as high-glycemic-index diets for their
73 propensity to raise blood glucose levels, high sugar diets have been linked to the increase in obesity with
74 particularly strong evidence for the consumption of sugary beverages (4).

75 Obesity is defined as a body mass index (BMI) greater than 30 and is a non-monolithic disease
76 caused by metabolic, genetic, socioeconomic, and environmental factors. It doubled in prevalence in
77 more than 70 countries between 1980 and 2015 and is epidemiologically linked to the increased
78 prevalence of type 2 diabetes, cardiovascular diseases, some neurodegenerative diseases, and surgical
79 complications including infections (5, 6). In one such neurodegenerative disease, Parkinson's disease
80 (PD), it has been reported that patients show higher total sugar and added sugar consumption than
81 healthy controls (7). Despite evidence of higher disease-concurrent intake in diagnosed individuals, it is
82 less clear how sugar diets influence the onset of PD (8).

83 PD is a late-onset neurodegenerative disorder characterized by loss of function and death in the
84 dopaminergic neurons of the substantia nigra region of the brain. PD impacts 1-3% of the global
85 population over age 65. Oxidative stress and mitochondrial dysfunction have both been identified as
86 potential causes or critical steps in the pathology of the disorder (9). Epidemiological studies
87 consistently find relationships between blood glucose levels, insulin intolerance, and PD. Though the

88 causal nature is unclear, increased blood glucose levels have been identified in drug-naïve patients and
89 those showing cognitive decline (10), and elevated blood glucose is a predictor of cognitive decline (11).
90 Increased added sugar intake has been associated with increased frequency of developing PD and
91 greater symptom severity and medication requirements post diagnosis (12).These same studies and
92 others have further found that decreased levels of insulin and increased insulin resistance were
93 associated with cognitive decline in PD patients (10, 11, 13). It has not been clearly established if
94 increased sugar intake and elevated blood glucose are causal or secondary to decreased insulin levels
95 and sensitivity to insulin.

96 To expand understanding of the complex relationship between high sugar diets, obesity, and
97 susceptibility to dopaminergic neurodegeneration, we turned to the nematode *Caenorhabditis elegans*.
98 *C. elegans* has been widely used as a model in biomedical research in general and to explore the impacts
99 of high-sugar diets in particular, because of its high genetic homology to humans, short life cycle, and
100 conservation of key pathways including insulin signaling (14). *C. elegans* fed high-glucose diets generally
101 demonstrate slower growth, decreased reproduction, shortened lifespan, neuronal and mitochondrial
102 dysfunction, decreased anoxia survival, and increased oxidative stress (15-19). High-fructose diets,
103 though less explored, have been shown to decrease lifespan and health span, induce mitochondrial
104 swelling, and decrease anoxia survival of worms (19, 20).

105 *C. elegans* has also been employed for studies of PD. Possessing 8 dopaminergic neurons and
106 high genetic tractability, several transgenics have been generated to assist with visualization of
107 dopamine neuron morphology (21, 22). High glucose exposure studies in *C. elegans* showed increased
108 susceptibility to organophosphate pesticide-induced neurodegeneration in dopaminergic, GABAergic,
109 and cholinergic neurons (17, 18, 23). These studies, however, were mostly performed with acute,
110 developmental exposures to glucose.

111 Here, we present evidence from worms fed chronic, not acute, 100 mM D-glucose or fructose
112 from day 1-day 5 of adulthood on the mechanistic relationships between high-sugar diets and
113 dopaminergic neurodegeneration. With this strategy, we have avoided the potential for confounding
114 effects of bioenergetic remodeling resulting from developmental mitochondrial stress (24-28). Doses
115 were selected to closely match the large body of literature in *C. elegans* studying high sugar diets, in
116 which 100 mM consistently produces clear effects but is non-lethal (Table 1). To improve upon the
117 common use of decreased fluorescence of the cell bodies within the cephalic (CEP) neurons in the head
118 of the worm as a proxy for degeneration, we employ a neurodegeneration scoring methodology with
119 improved ability to detect subtle changes to the neuronal processes. We not only assess whether high
120 sugar diets induce dopaminergic neurodegeneration, but whether they enhance susceptibility to the
121 canonical dopaminergic neurotoxicant 6-hydroxydopamine (6-OHDA). Upon entering the cell, 6-OHDA
122 increases oxidative stress partly through auto-oxidation, and partly through inhibition of mitochondrial
123 electron transport chain Complexes I and IV, resulting in decreased ATP levels, akin to two other PD
124 toxicant model toxicants, rotenone and MPP+ (29). Utilizing this method, we report that chronic, adult
125 high glucose or high fructose diets resulted in neuroprotection from 6-OHDA exposure. The impact of 6-
126 OHDA on redox state, not its effect on ATP levels, was abrogated by high sugar, suggesting that redox
127 alterations, not energetic alterations, underlie the dopaminergic neurotoxicity of 6-OHDA in *C. elegans*.
128 In absence of alterations to glutathione levels, redox tone, and antioxidant enzyme expression, we
129 suggest altered dopamine neurotransmission leads to decreased 6-OHDA uptake and prevents toxicity.

130 Results:

131 **Adult high sugar diets decrease lifespan and fecundity while increasing adiposity**

132 *C. elegans* has been used extensively to evaluate the impacts of dietary paradigms on lifespan and
133 reproduction. In the case of high sugar diets, previous work in *C. elegans* has focused largely on

134 exposures beginning in early development. To discern how adult glucose and fructose exposures impact
135 key biological functions, and permit comparison to previously published developmental exposure
136 studies, we first evaluated the impact of our adult exposure paradigm on adiposity, lifespan, and
137 fecundity. In concurrence with the effects observed with developmental sugar exposures, worms
138 transferred as young adults to nematode growth media (NGM) plates supplemented with 100 mM
139 glucose or 100 mM fructose show increased lipid accumulation represented by an 85.6% and 46.2%
140 increase in fluorescence intensity of an mCherry::mdt-28 fusion protein localized primarily to lipid
141 droplets (Fig 1A). Increased lipid stores were particularly concentrated throughout the intestine, around
142 the vulva, and to a lesser extent in the head. The effect was more intense in glucose fed worms than
143 fructose fed worms (Fig 1B). Similarly, and again in agreement with observations from developmental
144 exposures, worms fed glucose and fructose had a modest decrease in their average brood size from
145 297.7±7.9 eggs per worm to 247.9±7.9 and 272.7±4.8 respectively (Fig 1C). Beyond total brood size, the
146 time course of egg laying was altered such that both high sugar diets caused egg laying to be distributed
147 more evenly over days 1-3 of adulthood as opposed to most being laid the first 2 days with a sharp
148 decrease on the third (Fig 1D), which is the typical pattern on control plates. Finally, the sugar exposure
149 paradigm shows no significant lethality during exposure, but both sugars led to a significantly decreased
150 median lifespan post exposure (SFig 1, Fig 1E), with a greater decrease on fructose (6 days shorter than
151 control diet) than glucose (2 days shorter).

152 **High sugar diets protect from 6-OHDA induced dopaminergic neurodegeneration**

153 To define the role of high sugar diets in age-related and toxicant-induced neurodegeneration, we
154 compared dendritic degeneration in worms exposed to high sugar diets throughout reproductive
155 adulthood and subsequently exposed to either 25 mM or 50 mM 6-hydroxydopamine (6-OHDA). 6-
156 OHDA is a well-validated dopaminergic neurotoxicant transported into the dopaminergic neurons via
157 the DAT-1 transporter. The CEP neurons in *C. elegans* are easily visualized within the head of the worm

158 and have a well characterized damage phenotype including dendritic blebbing and breaking (21, 22, 30-
159 32). Using a qualitative scale in which increasing score represents increasing damage, we found that high
160 sugar diets did not increase age related neurodegeneration. In response to 25 mM 6-OHDA exposure
161 high glucose was protective, and both sugars were protective at the 50 mM dose with fewer instances of
162 broken and fully deteriorated sections of dendrite (Fig 2A, 2B, SFig 2).

163 **Neuroprotection by high sugar diets is not explained by alterations in mitochondrial amount or**
164 **morphology**

165 Next, we worked to understand the mechanism for the observed glucose and fructose
166 neuroprotection. As the 6-OHDA exposure paradigm is acute (one hour), we reasoned that the
167 mechanism of protection resulting from the chronic high sugar diet must be present when the exposure
168 begins. Both high glucose and high fructose diets have been previously associated with increased
169 mitochondrial swelling and fragmentation (20, 33). Increases or decreases in mitochondrial fission and
170 fusion dynamics are vital to cellular response to dietary and toxicant exposures (34, 35). Mitochondrial
171 fission is required for the increase in reactive oxygen species and induction of cell death by high glucose
172 diets in some cell types (36). Therefore, we evaluated mitochondrial morphology and number in the CEP
173 neuron dendrites and mitochondrial area in muscle cells to determine if clear differences in
174 mitochondrial dynamics were present prior to 6-OHDA exposure. No differences were apparent in the
175 muscle cell mitochondrial area (SFig 3) or in neuronal cell mitochondrial number (Fig 3A); however, high
176 glucose diets altered mitochondrial morphology within the CEP neurons (Fig 3B-3D). In CEP neurons,
177 high glucose diets resulted in small but significant elongation of the mitochondria from 1.832±0.04
178 micrometers to 2.005±0.05 micrometers in length (Fig 3A-B). Similarly, the maximum length of
179 mitochondria increased from 3.98±0.11 to 4.50±0.16 (Fig 3C). This resulted in an increase of total
180 mitochondrial length per dendrite from 16.45±0.32 micrometers to 18.64±0.45 micrometers (Fig 3D).
181 However, high-fructose diets did not result in any significant alterations to mitochondrial number or

182 morphology within the dendrites, indicating that even if glucose-mediated increased mitochondrial
183 length contributed to protection from 6-OHDA, fructose's protective effect could not be explained by
184 this mechanism. Continuing to assess mitochondrial mechanisms that could confer protection, we
185 moved to evaluate cellular and organismal bioenergetics.

186 **High sugar diets do not rescue ATP depletion caused by electron transport chain inhibition**

187 It has been theorized that ATP depletion may incite a negative feedback loop resulting in and enhancing
188 neurodegeneration (37, 38). Therefore, we next assessed whether the high sugar diets protected from
189 dopaminergic neurodegeneration by improving energetics at baseline, or upon challenge. On an
190 organismal level, we assessed mitochondrial bioenergetic function by whole worm respirometry. We
191 found a small increase in basal oxygen consumption rate (SFig 4); however, this is accounted for by
192 larger worm size. After accounting for worm size, we found no alterations to electron transport chain
193 function or non-mitochondrial oxygen consumption (Fig 4A). We also assessed whole-worm ATP levels
194 by luminescent assay and observed no baseline differences (Fig 4B). To assess energetic status upon
195 challenge, we exposed worms to the complex I inhibitor rotenone. This acute (1-hour) challenge
196 decreased whole-body ATP levels of sugar-fed worms 40% more than controls (Fig 4B). To determine if
197 energetic responses in the CEP neurons follow the same trend as the whole-organism responses, and
198 assess whether that susceptibility would manifest in the context of the 6-OHDA challenge that we used
199 for neurodegeneration, we exposed worms expressing the PercevalHR ATP:ADP ratio reporter in
200 dopaminergic neurons to 50 mM 6-OHDA and vehicle controls of ascorbic acid. Surprisingly, ATP:ADP
201 ratio within the CEP neuron soma was not different across diets before or after 6-OHDA exposure (Fig
202 4C). Notably, ascorbic acid, the vehicle for 6-OHDA, induced significant ATP depletion. As ascorbic acid
203 does not induce neurodegeneration, and both sugars protected from neurodegeneration without
204 protecting from ATP depletion, our results are inconsistent with ATP depletion causing degeneration of
205 the CEP neurons.

206 **High sugar diets minimally alter organismal antioxidant gene expression and do not change**
207 **glutathione concentrations**

208 The third mechanism we tested for sugar-mediated dopaminergic neuroprotection was upregulation of
209 antioxidant defenses. Acute high sugar diets have been demonstrated to increase oxidative stress;
210 however, more chronic exposure in young adults increased expression of the proteins glucose-6-
211 phosphate 1-dehydrogenase and glutathione disulfide reductase, which should allow for accelerated
212 reduction of glutathione and confer protection from oxidant exposures (39). We hypothesized that
213 chronic high-sugar diets might cause similar compensatory and protective upregulation of antioxidant
214 systems, which could combat redox stress induced by 6-OHDA exposure. First, we assessed if our
215 chronic high sugar diets altered organismal redox state using a whole-animal reduction oxidation
216 sensitive GFP (roGFP) construct that reports on the ratio of oxidized to reduced glutathione. Due to the
217 increase in autofluorescence at 405nm driven primarily by gut autofluorescence (Supp Fig 5A-B), we
218 restricted our analysis to the head region from the tip of the head of the worm to the end of the
219 terminal pharyngeal bulb. High sugar diets induced no differences in the redox tone of the glutathione
220 pool on an organismal level (Fig 5A). To ensure that the lack of alteration in glutathione redox state was
221 not due to differences in total glutathione pool sizes, we quantified total glutathione levels and found no
222 statistically significant difference (Fig 5B). To determine if this result, which was contrary to findings
223 from acute exposures, was due to altered antioxidant gene expression, we evaluated the mRNA
224 expression levels of multiple antioxidant enzymes. We observed slight (10-20%) decreases in expression
225 of the glutathione reductase encoding gene *gsr-1* in glucose fed worms, and of a cytosolic CuZnSOD
226 encoding gene, *sod-5,* in fructose fed worms (Fig 5C, SFig 6). Decreased expression of antioxidant genes
227 may lead to susceptibility to oxidant exposures, leading us to examine redox state specifically within the
228 mitochondria of the CEP neurons that were targeted by 6-OHDA in our neurodegeneration studies. We
229 utilized a CEP neuron-specific mitochondrial-targeted roGFP and, in accordance with the organismal

230 result, no difference was observed as a result of the high sugar diets alone. However, sugar-fed worms
231 had a significantly smaller increase in oxidation state after 6-OHDA exposure (Fig 5D). This result is
232 consistent with protection from neurodegeneration and of oxidative stress as a driver of
233 neurodegeneration. However, it could be explained either by a cell-specific increase in antioxidant
234 defenses, not detectable by our whole-organism measurements, or by a decrease in 6-OHDA uptake by
235 the dopaminergic neurons. We next tested the latter possibility.

236 **High sugar diets modulate the dopamine transport system to decrease dopamine reuptake**

237 6-OHDA is actively transported into the dopaminergic neurons by the DAT-1 transporter. Each worm has
238 only 4 CEP neurons, which makes direct quantification of the uptake of 6-OHDA impractical. Therefore,
239 we instead measured proxies for the quantity and activity of the DAT-1 transporter. We assessed mRNA
240 expression of *dat-1*, the re-uptake transporter responsible for 6-OHDA transport into the CEP neurons;
241 *cat-1*, a vesicular monoamine transporter critical to dopamine packaging and release (40); *cat-2*, which
242 encodes tyrosine hydroxylase, the protein that catalyzes the rate limiting step in dopamine synthesis;
243 and the dopamine receptor *dop-3* (Fig 6A). With no alterations in expression levels observed via rtPCR,
244 we also examined DAT-1 expression via a *dat-1* promoter driven GFP strain. We detected a 28.16±3.30%
245 and 26.03±3.15% decrease in *dat-1* promoter-driven fluorescence in glucose and fructose exposed
246 worms, respectively (Fig 6B). To further evaluate the functional status of dopaminergic
247 neurotransmission, we utilized a swimming induced paralysis (SWIP) assay. Release of dopamine into
248 the neuro-muscular junction dictates the ability of the muscle cells in worms to contract and relax.
249 When too much dopamine enters the junction, or not enough is cleared via re-uptake, the worms are
250 temporarily paralyzed. After 10 minutes of swimming, glucose and fructose fed worms were five and
251 two times more likely to SWIP (Fig 6C). Increased SWIP activity may indicate decreased dopamine
252 reuptake by the CEP neurons, which would protect against 6-OHDA uptake. To confirm the role of *dat-1*
253 in this phenotype, we performed the SWIP assay with worms possessing a 1836 base pair knock out (KO)

254 in *dat-1*. Unlike their response in early life, day 8 *dat-1* KO worms do not SWIP more than controls,

255 implying an adaptive response throughout life (SFig 7, Fig 6D). However, *dat-1* KO worms fed glucose

256 and fructose are also not susceptible to SWIP, supporting our hypothesis that DAT-1 downregulation or

257 internalization as a result of high sugar diets is the source of elevated susceptibility of sugar fed worms

258 to SWIP (Fig 6D). Together, these data support the overarching hypothesis that chronic sugar mediated

259 *dat-1* downregulation decreases 6-OHDA induced dopaminergic neurodegeneration.

260 Discussion:

Table 1: Summary of previous research on high glucose and high fructose diets in *C. elegans*

Article	Sugar	Dose (mM)	Exposure paradigm	Lifespan	Brood Size	Oxidative Stress	Locomotion	Lipid Content	Neurodegeneration
Alcantar-Fernandez (2018)(15)	G	20, 40, 80, 100	L1-L4	↓26-52%	⊘ F0 ↓ F1, F2	↑	-	↑2-3 fold	-
Salim (2014)(17)	G	111	L1-L4	↓32%	↓30%	-	↓18%	-	↑
Garcia (2015)(19)	G	3.5-111	D1 adults to end of assay	↓ (anoxic conditions)	-	-	-	↑	-
	F	3.5-111	D1 adults to end of assay	↓ (anoxic conditions)	-	-	-	-	-
Schlotterer (2009)(41)	G	40	D1 adult to end of life	↓ 2 days	-	↑ D15 adults	-	-	-
Lodha (2020)(20)	F	277.5	L4 to end of life	↓ 5%	-	-	↓ 52% D10 adults	-	-
Tauffenberger (2014)(42)	G	277.5	L4 to end of life	↓F0 ⊘ F1 and F2	↓ F0, F1, F2	↓ F0 F1 (enhanced juglone survival)	-	-	↑ F0

Zhu (2015)(43)	G	100, 200	L1-L4	↓29.0% and 30.8%	-	↑	-	↑ (strain VS29)	-
Seung-Jae Lee (2009)(44)	G	111	D1 adult to end of life	↓ 20%	-	-	-	-	-
Liggett (2015)(45)	G	250	L4 to end of life	↓30-40% hermaphrodite ↑10% males	-	-	↓ 43% hermaphrodites, 7% males (D14)	-	-
Teshiba (2016)(46)	G	10, 50, 100	L4 to end of life	-	⊘ 100	-	-	-	-
Alcantar Fernandez (2019)(16)	G	20, 40, 80, 100	L1 to L4	-	-	↑ in all	-	-	-
Zheng (2017)(47)	G	111	L1 to end of life	↓	-	-	-	↑	-
	F	55, 111, 555	L1 to end of life	↑ at 55 and 111 ↓ at 555	-	-	-	⊘ at 55 and 111 ↑ at 555	-
Ke (2021)(48)	F	55.5	L4 to assay or end of life	↓	-	-	↓	↑ D1 adults	-
Gatrell (2020)(49)	G	250	L4 to assay or end of life	↓	⊘	-	↓	-	⊘ polyQ aggregation
Beaudoin-Chabot (2022)(50)	G	111	Adult D1 or D5 to end of life	↓ D1 ↑ D5	-	↑ D1 and D5, measured at D10	↓ D1 ↑ D5 Measured after 24-hour exposure	-	-
Engstrom (2022)(51)	G	333	Either only as L4 or adult, or both	-	↓ if fed glucose as adult ⊘ if only fed glucose as L4	-	-	-	-

Mondoux (2011)(52)	G	100, 200, 300, 400, 500	L4 to assay	-	↓at all but 200 ⊘ at 200	-	-	-	-
Xiong Wang (2020)(53)	G	5 50 400 500 520	L1 to end of life for lifespan L4 to end of life for brood size	↑ 14.36-27.55% from 5-500 ↓ 35.69% at 520	⊘ 5-50 ↓ 400-520	-	-	-	-
	F	5 50 400 500 550	L1 to end of life for lifespan L4 to end of life for brood size	↑ 1.52-23.36% from 5-400 ↓ 0.36-1.15% at 500-550	↑ from 5-50 ↓ 400-550	-	-	-	-
Gusarov (2019)(39)	G	111	L4 to assay	↓ 28%	-	⊘ at baseline ↓ as it protects from oxidants	-	↑ at D3 adult	-
This work	G	100	D1-D5 of adulthood	↓	↓	⊘ at baseline ↓ as it protects from 6-OHDA	↓	↑	⊘ at baseline ↓ as it protects from 6-OHDA
	F	100	D1-D5 of adulthood	↓	↓	⊘ at baseline ↓ as it protects from 6-OHDA	↓	↑	⊘ at baseline ↓ as it protects from 6-OHDA

Summary of previous and current work studying the impact of high glucose and high fructose diets in *C. elegans*. Sugar: glucose (G) or fructose (F); ↓ represents a decrease, ↑ represents an increase, ⊘ represents no detected difference, and – represents endpoint not quantified

Sugars such as glucose and fructose are essential for animal life, but diets containing excessive sugar can increase neurodegeneration in mammalian models and *C. elegans* (18, 23, 49, 54). We expand on previous investigations of high sugar diets in *C. elegans* to investigate mechanistic links between high sugar in adulthood, mitochondrial disfunction, and dopaminergic neurodegeneration (Table 1). Although

266 our exposure paradigm begins in early adulthood, like previous work, it still led to decreased lifespan,
267 increased lipid accumulation, and decreased reproduction. Notably, the rapid onset of reproductive
268 changes is cohesive with previous reports demonstrating adult exposure leads to decreased progeny,
269 while beginning exposure at late-L4 likely drives the slowed time course of reproduction by altering
270 germline proliferation, meiotic entry, or sex differentiation(51). Despite these similarities, our results
271 were inconsistent with previous findings in which high glucose induced degeneration of dopaminergic
272 neurons, decreased dopamine levels, and exacerbated monocrotophos-induced neurotoxicity (18, 55).
273 In this study we did not find a change in neurodegeneration after chronic, adult high-glucose and high-
274 fructose diets. Rather, we found that these diets protected from 6-OHDA-induced dopaminergic
275 neurodegeneration. After assessing a number of potential mechanisms of protection, we propose that
276 the protective effect is mediated by decreased 6-OHDA uptake via the DAT-1 transporter.

277 Contrary to previous work showing electron transport chain impairment and severe
278 mitochondrial dysfunction (16, 20, 54), we only identified a slight elongation of the mitochondria in
279 dopaminergic neurons of glucose fed worms, and no change in those fed fructose. No difference in
280 mitochondrial function was detected with whole worm respirometry, total ATP levels, or ATP:ADP ratio
281 within the CEP neurons. The only apparent indication of bioenergetic dysfunction induced by the high
282 sugar paradigm was in response to challenge by the Complex I inhibitor rotenone, which caused nearly
283 40% greater ATP depletion in sugar-fed worms. 80 mM and 100 mM glucose dose-dependently
284 decreased the activity of Complex I in a previous *C. elegans* study, without alteration to ATP, ADP, or
285 AMP concentrations (16). It is plausible that lower Complex I activity decreased the dose of rotenone
286 required to completely inhibit Complex I function, or that glycolysis is already enhanced by the high
287 sugar diets, preventing further transition to glycolytic metabolism. We previously demonstrated the
288 upregulation of glycolysis in rotenone-treated worms (56) , though not in the context of high-sugar
289 diets. Because different cell types rely on different bioenergetic pathways, we next tested whether the

290 increased susceptibility to acute electron transport chain inhibition we observed on the organismal level
291 would also be observed within the CEP neurons. Remarkably, sugar-fed worms showed no discernable
292 difference in ATP:ADP ratio after 6-OHDA exposure, which is inconsistent with energetic deficit causing
293 neurodegeneration, since the same sugar exposures protected against 6-OHDA-induced
294 neurodegeneration. Furthermore, as the vehicle in our neurodegeneration experiments also decreases
295 ATP:ADP ratio but did not cause neurodegeneration, it is improbable ATP depletion is the mechanistic
296 step responsible for 6-OHDA induced dopaminergic neurodegeneration. Earlier work characterizing
297 rotenone similarly noted that redox stress, not ATP depletion, is critical for its induction of
298 neurodegeneration (57, 58).

299 Previous studies with acute sugar exposure models have detected increased antioxidant enzyme
300 expression or increased total glutathione levels (15, 39), which would protect from the oxidative stress
301 induced by 6-OHDA. However, we found no large differences in total glutathione, redox tone of the
302 glutathione pool, or expression of antioxidant enzymes in the glutathione-related, superoxide
303 dismutase, catalase, peroxiredoxin, or thioredoxin families. It is possible that differences in mRNA
304 and/or protein levels specifically within the CEP neurons existed but were not detected in our whole-
305 organism gene expression analysis. However, many previous studies that detected upregulated
306 antioxidant defenses after acute exposures also employed whole-organism measures, making this
307 explanation less likely. Perhaps more likely, our chronic exposure paradigm may result in adaptations
308 across the lifetime of the worm in glucose uptake, transport, and utilization, culminating in a loss of the
309 acute-phase oxidative stress response, explaining our lack of effects. Thus, despite finding a decreased
310 redox response to 6-OHDA in the CEP neurons of sugar-fed worms, this resilience to oxidative challenge
311 is unlikely a result of enhanced antioxidant defenses. Having failed to find compelling evidence for redox
312 changes or bioenergetic inhibition as the mechanism for neuroprotection, we next considered the
313 possibility of altered 6-OHDA uptake in high-sugar fed worms.

314 The DAT-1 transporter is required for 6-OHDA uptake into the CEP neurons, and inhibition of
315 DAT-1 is protective from 6-OHDA induced degeneration (31, 32). *dat*-1 mutants were among the earliest
316 to be identified as sensitized to swimming induced paralysis (SWIP), and synaptic localization of DAT-1 is
317 required to prevent SWIP (59). Our observation of increased tendency towards SWIP after sugar
318 exposure is consistent with modified dopamine transport, and is confirmed by the loss of the SWIP
319 phenotype in sugar-fed *dat-1* KO worms. This could be an attempt to maintain dopamine in the synaptic
320 cleft despite lower total dopamine levels, a possibility bolstered by recent evidence that high glucose
321 diets decrease dopamine levels (55). Though little work has explored the relationship between DAT-1
322 and high sugar diets, we report a nearly 30% decrease in *dat-1* promoter-driven GFP fluorescence.
323 Though this decrease was smaller than that reported in recent work in *C. elegans* demonstrating an 80%
324 decrease after high-glucose exposure, these combined findings support a relationship between high
325 sugar diets and modulation of dopamine transmission in *C. elegans* (55). In mammalian models, high
326 glucose diets activate protein kinase C, which drives DAT endocytosis, opening the possibility for a
327 similar high sugar driven effect in worms (60-62). Notably, alterations to SWIP were not associated with
328 increased neurodegeneration.

329 Beyond the toxicant-induced neurological impacts, we also deepen understanding of how the two most
330 consumed sugars compare in their biological effects. High-glucose and high-fructose diets in our study
331 produced similar but non-identical effects in nearly all experiments. Only glucose-fed worms exhibited
332 elongated neuronal mitochondria, and in general, apart from lifespan, fructose-fed worms typically
333 showed a less significant departure from controls than glucose-fed worms. These discrepancies may be
334 explained by differences in the metabolism of these sugars, but it remains clear that the pathways
335 driving alterations in dopaminergic function, lifespan, reproduction, and ATP production are impacted in
336 very similar ways. This may indicate that in models with more complex organ systems, where stronger
337 differences between sugar types have been observed, those differences are driven by tissue-specific

338 metabolism and responses. For example, fructokinase, fructose bisphosphate aldolase-B, and
339 dihydroxyacetone kinase, the three enzymes responsible for fructose metabolism, are only found in the
340 liver and kidney of rats (63). In *C. elegans*, hexokinases (HXK-1,2,3) predicted to carry out the first step in
341 fructose metabolism, are expressed ubiquitously (64). Thus, the reported mitochondrial swelling and
342 respiratory dysfunction induced only by fructose in rat livers may be a result of specific mitochondrial
343 dynamics and concentrated fructose metabolites in the liver and kidneys, versus the potentially non-
344 tissue-specific metabolism in worms (65). It should be noted, in the same study in rats, high sugar diets
345 had generally similar effects on fatty acid oxidation and mitochondrial protein acetylation in isolation,
346 but divergent effects when supplemented on top of a high fat diet (65). Thus, further examination of
347 dietary components in isolation and combination will be required to understand the complex dynamics
348 governing effects of different sugars and how they relate to other model organisms.

349 The interaction between diet and toxicant exposure remains an active area of investigation due
350 to the plethora of dietary alterations and chemicals that currently occur (66-71). High sugar diets elicit
351 several metabolic and oxidative stress pathway alterations, depending on the exposure paradigm,
352 leading to interactions with toxicants that target the same pathways. In *Drosophila melanogaster*, high
353 glucose enhances Bisphenol A toxicity by exacerbating downregulation of testis-specific genes and
354 upregulation of ribosome-associated genes (71). In *C. elegans*, high sugar diets increase susceptibility to
355 monocrotophos and parathion, including increasing the damage inflicted on dopaminergic neurons (17,
356 18, 72). We show that both high-glucose and high-fructose decrease susceptibility to 6-OHDA induced
357 neurodegeneration but enhance susceptibility to rotenone induced ATP depletion. Together, these data
358 highlight the critical need to continue assessing toxicant by diet interactions for multiple endpoints, as
359 the outcomes are likely highly specific to the tissue of interest and toxicokinetics of each chemical used.

360 There are also limitations to our study. We do not address how ecologically relevant
361 neurotoxicants would interact with high sugar consumption. Due to the unique toxicokinetic effect of

362 DAT-1 on 6-OHDA uptake, which would not generally be conserved for other dopaminergic toxicants,
363 impacts of high sugar should be examined not only with ecologically relevant pollutants, but toxicants
364 with varied mechanisms of toxicity. It is also possible the mechanisms we observe are limited to our
365 exposure paradigm. As shown in Table 1, previous investigations often rely on developmental acute
366 exposures and show different neurodegenerative results. Further work is required to understand the
367 patterns of redox, bioenergetic, and dopaminergic transmission changes that occur both as a function of
368 age and sugar consumption.

369 Conclusions:

370 Adult high-glucose and high-fructose diets are protective against 6-OHDA induced dopaminergic
371 neurodegeneration, potentially due to their modifications of dopamine transmission processes
372 decreasing 6-OHDA uptake. Intriguingly, this protection occurs despite decreased lifespan, decreased
373 fecundity, and increased lipid storage. As demonstrated by the lack of neurodegeneration induced by
374 ATP depletion, the induction of oxidative stress appears to be more important in the induction of
375 dopaminergic neurodegeneration by 6-OHDA. This study highlights the important interactions between
376 lifestyle factors such as diet, oxidative stress, and susceptibility to toxicant induced dopaminergic
377 neurodegeneration.

378

379

380 Materials and Methods:

381 Strains and Culture

382 The wild-type CGC (N2), LIU2 (Idrls[mdt-28p::mdt-28::mCherry + unc-76(+)]), BY200 (pdat-1:GFP),
383 JMN080(pdat-1::MLS::GFP), SJ4103 (pmyo-3::mitoGFP), JV2 (*jrls2*[rpl-17p::Grx-1-roGFP2+unc-119(+)]),
384 PE255 (*feIs5*[sur-5p::luciferase:GFP+rol-6(su1006)]), and PHX2923 (pdat-1::PercevalHR), PHX2867 (pdat-
385 1::MLS::roGFP), RM2702 (dat-1(ok157), were maintained at 20 C on K-agar plates seeded with OP50 *E.*
386 *coli*. For experiments, worms were synchronized through egg-lays as in which worms were transferred
387 onto new plates, allowed to lay eggs for 3 hours, then washed to remove adults. They were aged to
388 adulthood on K-agar plates seeded with OP50 *E. coli*. As D1 adults (72 hours post egg lay), worms were

389 evenly split between NGM, NGM + 100 mM glucose, or NGM + 100 mM fructose plates freshly seeded
390 with OP50 E. coli. They were transferred daily to freshly seeded plates to discount effects of plate
391 acidification. All worms were reared from D1-D5 of adulthood on their respective group plate (control,
392 glucose, or fructose). On D8 assays were run, initiated, or worms were returned to K-agar OP50 plates as
393 described for individual assays.

394 Generation of transgenic strains

395 *Generation of dat-1p::MLS::GFP*

396 To generate the *dat-1*p::MLS::GFP plasmid, a 886 bp fragment directly upstream of the dat-1 start codon
397 was amplified from wildtype (N2 Bristol type) genomic DNA, using primers with overhangs that
398 contained homology to a plasmid containing a mitochondrial localization sequence (MLS) and GFP,
399 Forward Primer 5'→3': agggcgaattgggtaccCGTCTCATTCCTCATCTCCGAGC and Reverse Primer: 5'→3':
400 GTGCCATatcgatGGCTAAAAATTGTTGAGATTCGAGTAAACCG. The mitochondrial localization sequence was
401 originally amplified from Fire Vector pPD96.32. pPD96.32 was a gift from Andrew Fire (Addgene plasmid
402 # 1504 ; http://n2t.net/addgene:1504 ; RRID:Addgene_1504). The amplified dat-1 promoter was
403 inserted into the plasmid containing the MLS and GFP using Gibson Assembly and insertion was
404 confirmed by colony PCR with a nested GFP reverse primer and M13 Forward primer. The plasmid was
405 sequenced to check for any mutations and co-injected with 50 ng/µl unc-119 rescue DNA, 50 ng/µl
406 pBsSK, and 50 ng/µl EcoR1 cut salmon sperm DNA into unc-119(ed4) hermaphrodites. Once
407 extrachromosomal lines were established and dat-1p::MLS::GFP signal was observed, plasmid was
408 integrated by gamma irradiation as previously described (73). Integrated lines were outcrossed with N2
409 to remove possible background mutations.

410 *Generation of dopaminergic neuron PercevalHR and mitochondrial roGFP*

411 Worm strains expressing mitochondrial targeted reduction oxidation sensitive GFP (roGFP) and
412 PercevalHR within the dopaminergic neurons were generated by SunyBiotech
413 (https://www.sunybiotech.com). Both constructs were cloned into the pPD95.77 vector and included
414 890 bp of the *dat-1* promoter (ending just upstream of the start codon) amplified from genomic DNA
415 and the 5'UTR from the *unc-54* gene present in the pPD95.77 vector. We inserted the reporter genes
416 immediately downstream of the *dat-1* promoter and upstream of the *unc-54* 5'UTR. The mito-roGFP2-
417 Grx1 coding sequence was adapted from pUAST mito roGFP2-Grx1 (Addgene Plasmid# 64995) by codon
418 optimizing for expression in *C. elegans* using the *C. elegans* Codon Adapter (74) and a single intron was
419 added 402 bp downstream of the start codon. The Perceval-HR coding sequence was adapted from
420 pRsetB-his7-Perceval (Addgene Plasmid# 20336) by codon optimizing for *C. elegans* expression and a
421 single intron was added 444 bp downstream from the start codon. The construction of the plasmids,
422 verification by sequencing, microinjection into animals, integration, and isolation of individual strains
423 were performed by SUNY Biotech. We received three low-copy-number strains for each construct, and
424 all three strains were phenotypically normal.

425

426 Fluorescence Microscopy

427 Strain and specific image analysis details are listed below for each individual endpoint. However, all
428 strains were imaged with a Keyence BZX-2710 microscope. Unless otherwise specified, worms were

429 transferred by stainless steel pick to 2% w/v agarose pads, anesthetized with 15-20 uL 0.5 M sodium
430 azide, and imaged immediately. All quantitative image analysis was performed using Fiji ImageJ
431 software. Background subtraction was performed for all quantitative microscopy by subtracting the
432 equivalent measurement (mean grey value, etc) of a region in the image without a worm present.

433 Fat Quantification

434 After 5 days of dietary exposure, LIU2 worms were washed off plates and washed three times with K-
435 medium to remove bacterial debris. Worms were visualized in brightfield and under and EGFP or
436 TexasRed filter with a 10X objective. Three independent experiments were conducted, with
437 approximately 20 worms per treatment group imaged in each. Worm bodies were outlined as the region
438 of interest (ROI) and mean grey value was determined within the full body of the worm.

439 Lifespan

440 Lifespan assays were carried out with few modifications from previous descriptions (source). After 5
441 days of dietary exposure, 50 BY200 transgenic worms from each treatment group were transferred to 6
442 cm K-agar plates seeded with OP50. Worms were transferred to fresh plates every third to fourth day
443 and monitored daily for death. Worms were considered dead if they displayed no touch response when
444 poked with a steel pick and no bodily movement was observed. Animals that crawled off the plate or
445 died due to vulval protrusion or bagging were censored. The data is represented as starting on day 8 as
446 only worms that were alive on day 8 were used for subsequent analysis.

447 Reproduction

448 Single worms were transferred to individual 6 cm NGM or NGM + sugar plates as late L4. They were
449 transferred to a second plate 48 hours later, then were transferred every 24 hours to the remaining
450 plates. Progeny were counted 48 hours after the adult was removed. At least 5 worms per treatment
451 were utilized in each of three biological replicates.

452 Dopaminergic Neurodegeneration

453 *Exposure and Imaging*
454 On day 5 of dietary exposure, worms were washed and dosed with 25 mM or 50 mM 6-
455 hydroxydopamine (6-OHDA) in 10 mM or 20mM Ascorbic Acid (AA) solution [Ascorbic Acid, K+ mixture
456 (K-medium, Cholesterol, $CaCl_2$, $MgSO_4$)]. Control groups were incubated in an identical volume of only
457 the AA solution. All groups were incubated for 1 hour with rocking and subsequently washed with K-
458 medium solution three times to ensure complete removal of 6-OHDA. They were replated on K-agar
459 plates seeded with 2X OP50 and incubated at 20 C for 48 hours prior to imaging. Images were obtained
460 with the 40X objective in Z-stacks encompassing the full head of the worm. Images were processed by
461 generating maximal value Z-projections of stacks with FIJI ImageJ software and cropped to only display
462 the head region of a single worm per image.
463
464 *Scoring*
465 Images were blindly scored with the open access software Blinder, by Solibyte solutions (75). Each
466 dendrite of the four CEP neurons of each worm were scored on a scale of 0-4, as follows:
467 0- no visible damage or abnormalities
468 1-blebs or kinks encompassing less than 50% of the dendrite
469 2-blebs or kinks on encompassing more than 50% of the dendrite

470 3-breaks present with more than 50% of the dendrite remaining
471 4-breaks present with less than 50% of the dendrite remaining
472 To ensure scoring validity, the built-in Quality Control feature was utilized, and images were rescored
473 until the error was less than 15%. Statistical significance was quantified by chi-squared test with a
474 Bonferroni corrected p-value. Due to the high number of comparisons, letters are used to demonstrate
475 results of pairwise comparisons. Statistically significant differences are represented by no overlapping
476 letters when comparing two bars.
477

478 Seahorse Analysis

479 On day 5 of dietary exposure, whole worm respirometry was performed with a Seahorse Xf^{e}24
480 Extracellular flux analyzer as previously described (76), with the following modifications: Worms were
481 diluted to approximately 30 worms per well to maintain optimal oxygenation of the well during the
482 protocol and 40 uM DCCD was utilized to obtain maximal inhibition of mitochondrial electron transport
483 chain Complex V. 100-500 worms were reserved from each replicate and immediately imaged on K-agar
484 plates for size determination. Worm volume was quantified using the WormSizer ImageJ plugin for
485 normalization to worm volume.

486 Mitochondrial Morphology

487 On Day 5 of adulthood, strains SJ4103 and JMN080 worms were imaged with the 60X and 40X objectives
488 respectively. Images were taken as z-stacks encompassing the full muscle cell and maximally projected
489 for analysis in ImageJ. CEP neuron mitochondria were analyzed for the number and length of each
490 mitochondrion within each dendrite by using the line tool to manually trace each mitochondrion. Body
491 wall muscle mitochondria were analyzed for mean grey value per muscle cell as a proxy for total
492 mitochondrial mass.

493 Swimming Induced Paralysis

494 On day 5 of the dietary exposure protocol approximately 10 worms were picked by flame sterilized steel
495 pick into 100 uL of Millipore water in one well of a 96 well plate, each well was recorded for a minimum
496 of 10 minutes from the time the pick was removed from the water. Videos were analyzed for the
497 percentage of worms paralyzed at one-minute intervals for ten minutes, starting from the time the pick
498 entered the water. Worms were considered paralyzed when they were completely rigid for 5 second
499 intervals before and after the one-minute mark.

500 Autofluorescence

501 On day 5 of dietary exposure, Bristol N2 worms were imaged with the 10X objective under brightfield,
502 405 nm, and 488 nm excitation. The brightfield image was used to select the entire body of the worm as
503 the ROI and fluorescence was quantified in each respective channel as mean grey value.

504 roGFP and PercevalHR imaging

505 On day 5 of dietary exposure, dat-1p::MLS::roGFP or JV2 worms, were paralyzed with 1 mM levamisole
506 HCl and imaged. PercevalHR was mounted on 5% w/v agarose pads and imaged without paralytics. JV2
507 was imaged with the 10X objective and both dopaminergic strains were imaged with the 40X objective

508 at 405 nm and 488 nm excitation. Mean grey value was quantified and compared in as a ratio or
509 405/488 for roGFPs and 488/405 for PercevalHR.

510 qPCR

511 On day 5 of dietary exposure RNA was extracted via the Qiagen RNeasy Mini Kit (Qiagen 74104). Briefly,
512 100-200 worms were collected into conical tubes in K-medium. All animals were shaken for 10 minutes
513 on an orbital shaker to clear gut bacteria, transferred to a 1.5 mL microcentrifuge tube, and suspended
514 in RLT buffer. Samples were immediately flash frozen in liquid nitrogen and thawed on ice. Disruption of
515 the worm cuticle was then completed by bead beating with zirconia beads for 8 cycles of 30 seconds
516 beating and 1 minute on ice. Homogenate was then utilized in accordance with kit instructions. cDNA
517 was synthesized from 2 ug total RNA with a high-capacity cDNA Reverse Transcription Kit in 20 uL
518 reactions (Thermo Fischer, Ref. 4368814). We carried out qPCR using diluted cDNA, Power SYBR Greeen
519 Master Mix (Thermo Fischer 4368702) and 0.5 µM of gene-specific primers (Sup Table 1) in a CFX96
520 qPCR Real-Time PCR module with C1000 Touch Thermal Cycler (BioRad). After 10 minutes at 95°C, a
521 two-step cycling protocol was used (15 seconds at 95°C, 60 seconds at 60°C) for 40 cycles. We calculated
522 relative expression using the ΔΔCt method with *cdc-42* and *tba-1* as reference genes. Genes only
523 expressed in the dopaminergic neurons, *dat-1*, *dop-3*, and *cat-2*, required an additional 10 cycles of PCR
524 amplification prior to qPCR for adequate detection. Three samples were recorded for each treatment for
525 each biological replicate. Three biological replicates were performed. Any data point for which the
526 standard deviation between three technical replicates was not below 0.300 was discarded. Due to the
527 low transcript levels of some antioxidant genes, fewer samples were valid for these genes.

528 Total GSH levels

529 On day 5 of dietary exposure, 200 worms from each group were suspended in 75 uL of MES buffer in 1.7
530 mL conical tubes. Approximately 50 uL 0.5 mm zirconium oxide beads were added to each tube. Samples
531 were homogenized via bead beating (8 cycles, 30s on sonication, 30s without sonication at 4 C). Next, 65
532 uL of homogenate was recovered, with 10 uL transferred to a new tube for protein quantification and 55
533 uL diluted by half with 5% w/v metaphosphoric acid for total GSH quantification. GSH quantification was
534 completed in accordance with instructions for tissue homogenate (Cayman Chemical Kit No.703002).
535 Protein quantification for each sample was conducted by BCA Assay in accordance with kit instructions
536 (Millipore Sigma 71285M).

537 Whole Worm ATP Levels

538 Strain PE255 worms were reared in accordance with the dietary exposure protocol, challenged with 20
539 uM rotenone for 1 hour, and transferred to 96-well plates for Luciferin-based ATP quantification as
540 previously described (77). Luminescence was normalized to number of worms per well rather than GFP
541 due to autofluorescence differences.

542

543 p*dat-1*::GFP fluorescence quantification

544 Strain BY200 worms were reared in accordance with the dietary exposure protocol. On day 8, worms
545 were picked onto 2% w/v agarose slides and paralyzed with 60 mM sodium azide. Images of the head

546 region of each worm were taken in z-stacks with 0.5 uM pitch such that the full cell body was captured.
547 Z-stacks were maximum projected and assessed for mean grey value in FIJI ImageJ software.

548 Graphing and Statistical Analysis

549 GraphPad Prism version 9.5.0 was used for all graph generation and statistical testing. Statistical tests
550 are identified in the figure legend of each graph.

551

552

553

554

555 Figure Legends:

556 Figure 1. High-sugar diets increase lipid content, decrease reproduction, and shorten lifespan. **A** Fat
557 quantification and **B** representative images of 8-day old LIU2 worms reared on control (n=77),100 mM
558 glucose (n=83), or 100 mM fructose (n=74) supplemented NGM plates with OP50 as a food source. **C**
559 Total number of progeny (n=15 per treatment) **D** progeny laid per day (n=45, 15 per treatment, p-
560 interaction<0.0001) of individual worms plated on 6 cm control or sugar supplemented plates from late
561 L4 to post-reproductive age. **E** Lifespan analysis of worms treated from days 1-5 of adulthood on control
562 (n=141, median survival 23 days), glucose (n=146, median survival 21 days, p=0.0271), or fructose
563 (n=137, median survival 17 days, p=0.0001) supplemented NGM plates then transferred to K-agar OP50
564 plates until death. Only worms that were alive on day 5 of adulthood were utilized. For **A-D**, Three
565 biological replicates were performed for each experiment. Shapiro Wilks normality tests were used to
566 confirm distribution normality of the data. One-way ANOVA followed by Tukey's Post-Hoc was used for
567 A and C to determine p-value. For D, a two-way ANOVA with Tukey's post-hoc was used. For **E**, a Kaplan-
568 Meier survival analysis was performed in conjunction with the Log-rank test. *p<0.0332, **p<0.0021,
569 ***p<0.0002, ****p<0.0001

570 Figure 2. High-sugar diets do not induce neurodegeneration and protect from the neurotoxicant 6-
571 hydroxydopamine (6-OHDA). **A** Representative images for each of the 5 scores used to assess
572 dopaminergic neurodegeneration. The ">" symbol in the score of a 1 denotes a bleb, and the "*" in the
573 score of a 3 denotes a break. **B** A comparison of neurodegeneration in control, glucose-fed, and
574 fructose-fed worms treated with a vehicle control of 5 mM Ascorbic Acid or 25 mM or 50mM of 6-
575 OHDA. Pairwise chi-squared analysis was run with a Bonferroni corrected p-value of < 0.003571 to
576 account for 14 pairwise comparisons. Statistical difference is represented by letters a-e such that bars
577 possessing the same letter are not statistically different, and bars possessing none of the same letters
578 are statistically different. Data from 6 biological replicates is represented for total n=2,676, n per group
579 =172-512.

580 Figure 3. High-glucose diet induces mild neuronal mitochondrial elongation. **A** The number of
581 mitochondria per dendrite, **B** average length of mitochondria per dendrite, **C** length of the longest
582 mitochondria per dendrite, and **D** sum of the lengths of all mitochondria within a dendrite in worms
583 reared on control (n=249), 100 mM glucose (n=127), or 100 mM fructose (n=134) supplemented NGM
584 plates. **A-D** Three biological replicates were performed. Shapiro-Wilks Normality tests determined all

585 data sets were non-normally distributed. Kruskal-Wallis test followed by Dunn's multiple comparisons
586 testwas used to establish p-values. *p<0.0332, **p<0.0021, ***p<0.0002, ****p<0.0001

587 Figure 4. High sugar diets do not alter baseline bioenergetics or protect from ATP depletion from
588 mitochondrial inhibitors. **A** Whole worm respirometry was performed on D8 worms after high-sugar diet
589 exposure to quantify mitochondrial respiratory function. Oxygen consumption rate was normalized to
590 worm number and volume to account for differences in body size. **B** Whole worm ATP levels were
591 quantified after dietary exposure to either control, high-glucose, or high-fructose conditions. Control,
592 glucose, and fructose exposed worms were also subjected to a 1-hour 20 uM rotenone challenge to
593 assess organismal response to electron transport chain inhibition. **C** Worms expression dat-
594 1::PercevalHR were exposed to control, high-glucose, or high-fructose conditions, and assessed on day 8
595 under after exposure to ascorbic acid or 50 mM 6-OHDA. *p<0.0332, **p<0.0021, ***p<0.0002,
596 ****p<0.0001

597 Figure 5. High-sugar diets protect from 6-OHDA induced oxidative stress minimal alteration to
598 antioxidant systems. **A** The redox tone of the glutathione pool was quantified to assess organismal
599 oxidative stress. Worms expressing reduction:oxidation sensitive GFP were reared from day 1-5 of
600 adulthood on NGM plates or NGM supplemented with 100 mM glucose or fructose. Control worms were
601 exposed to 3% H2O2 as a positive control for increased oxidation. Three biological replicates were
602 assessed with n: Control=33 Glucose=58 Fructose=40 H_2O_2=24 **B** Organismal total glutathione levels
603 were assessed control, glucose, and fructose fed worms. Three biological replicates were utilized with 2-
604 3 technical replicates averaged to produce n=1 per biological replicate. **C** Alterations to mRNA levels of
605 multiple families of antioxidants were assessed for alterations by qPCR. Three biological replicates were
606 performed with n=3 per replicate, total n=9 per treatment. **D** To examine redox response within the CEP
607 neurons to 6-OHDA, worms expressing *dat-1*::mls roGFP were used and exposed to control, vehicle (5
608 mM Ascorbic Acid) or 50 mM 5-OHDA on day 5 of adulthood. Three biological replicates are represented
609 with total n=195 **A-B** Normality was confirmed by a Shapiro-Wilks normality test; One-way ANOVA
610 followed by Tukey's Post-hoc was used to determine p-values. **C** Relative gene expression was
611 determined by the ΔΔCt method, and each gene was analyzed by one-way ANOVA with Tukey's Post-
612 hoc. **D** One-way ANOVA followed by Tukey's Post-hoc was used to determine p-values. For all panels
613 *p<0.0332, **p<0.0021, ***p<0.0002, ****p<0.0001

614 Figure 6. Dopamine transmission is altered in sugar-fed animals. **A** Relative expression of dopamine
615 synthesis, reuptake, and transporter genes was assessed via qPCR in worms reared on control NGM or
616 high-glucose or high-fructose supplemented plates. A one-way ANOVA with Tukey's post hoc was used
617 to determine p-values. **B** Quantification of pdat-1::GFP fluorescence intensity was assessed as a broader
618 measure of dat-1 transcription. Results represent three biological replicates, n=157, 112, 129
619 respectively. These data are non-normally distributed (Shapiro-Wilk's Normality p<0.05) and were
620 evaluated by a Kruskal-Wallis test, ****p<0.0001. **C** The tendency of sugar fed worms to undergo
621 swimming induced paralysis (SWIP) was determined. A two-way ANOVA with Dunn's post hoc was used
622 to assess significance. Four biological replicates are represented, n=12 for each diet. *p<0.0380,
623 **p<0.0002 **D** The tendency of *dat-1* KO worms to undergo SWIP compared to BY200 controls under
624 control and high-sugar diet conditions. Three biological replicates are represented, n=6 for each
625 treatment.

626 Supplementary Figure 1. Survival of worms during the 5-day exposure to high sugar. BY200 worms were
627 reared to Day 1, at which point 20 worms per treatment per replicate were transferred to control NGM
628 plates or plates containing 100 mM glucose or 100 mM fructose. Each day worms were assessed for
629 survival by touch response with a flame sterilized platinum pick. Surviving worms were transferred to
630 freshly seeded plates each day to avoid plate acidification and to separate them from progeny. For each
631 group 3 biological replicates were assessed, with 20 individuals per replicate. A two-way ANOVA was
632 performed to assess statistical significance, with no differences identified.

633 Supplementary Figure 2. P-values for individual chi-squared tests for analysis of dopaminergic
634 neurodegeneration. Chi-squared tests were used to determine the outcome of 15 comparisons with a
635 Bonferroni corrected p-value of 0.0033. Within each diet, the vehicle was compared to both doses of 6-
636 OHDA. Across diets each treatment was compared. Results are color coded for clarity: grey was not
637 assessed, green is statistically significant, yellow is not statistically significant

638

639 Supplementary Figure 3. Muscle cell mitochondrial mean grey value. SJ4103 worms were reared in
640 accordance with the dietary exposure protocol and imaged on day 8. Images were obtained using a
641 Keyence BZ-X710 with 60X magnification (oil immersion). Z-stacks were set to encompass the entirety of
642 the cell, and maximum projected for analysis. Individual cells were outlined as the region of interest for
643 analysis in Image J. Mean grey value was used as a proxy for total mitochondrial area (One-way ANOVA).

644 Supplementary Figure 4. Oxygen consumption rate normalized to worm number without accounting for
645 worm size. Whole worm respirometry was performed with the Seahorse XF24 Bioanalyzer and reported
646 as oxygen consumption rate normalized to the number of worms in each well. All wells from the same
647 biological replicate were averaged to produce n=1 (One-way ANOVA, Tukey's Post Hoc, *p<0.0332).

648 Supplementary Figure 5. Autofluorescence quantification at 488 nm and 405 nm excitation wavelengths.
649 N2 (wild-type) worms were reared on their respective sugar diets and imaged at day 5 of adulthood to
650 determine if high sugar diets alter worm autofluorescence. No significant difference was detected in the
651 N2 strain at 488 nm, however both high glucose and high fructose diets increase autofluorescence at
652 405 nm excitation (One way ANOVA, Tukey's Post Hoc,**p<0.0021,****p<0.0001)

653 Supplementary Figure 6. Relative gene expression of individual genes.

654 Supplementary Figure 7. Swimming Induced Paralysis Timecourse. BY200 worms were synchronized by
655 timed egg lay and assessed for susceptibility to swimming induced paralysis at times correlating to
656 various developmental and reproductive stages: 24-hours (L2 larval stage), 48-hours (L4 larval stage),
657 72-hours (early adults), 120-hours (mid-reproductive age adults), 168-hours (late-reproductive age
658 adults), and 192-hours (post-reproductive, experiment timepoint). Three biological replicates were
659 assessed for 24-168 hours, with 2 wells containing approximately 10 individuals each per replicate (n=6
660 per strain, per timepoint). The data for 192-hours is the data represented for D8 in figure 6D. Results
661 were assessed by two-way ANOVA followed by Sidak's Test for multiple comparisons with (p<0.05) as
662 the threshold for significance. Only the 48-hour (L4) timepoint indicated a significant difference,
663 p<0.0001.

664

665 Supplementary Table 1. Primers utilized for RT-qPCR

Gene	Forward (5'-3')	Reverse (5'-3')
cat-2	GGCGTTAGAGTTCAAGTTTGGT	CCGCTGTCAAAACCTTCTCC
cdc-42	GAGAAAAATGGGTGCCTGAA	CTCGAGCATTCCTGGATCAT
ctl-1,2,3	ACTAAAGTTTGGCCACACGG	CTTGGAGCATCTTGTCTGGC
dat-1	TTTTGCCATCCGGGTAGAGTC	GACATTGCTCTTTCCCTCTTCG
dop-3	CTTCTTGCTCGCTCTCGTTG	TGGAAGAGAACGATGAATGCG
gcs-1	ACAAGCCGAAGAGCAGGTGAATG	GCAAGCGATGAGACCTCCGTAAG
gsr-1	CGGATTTGATGTGACGCTTA	AAAGTTGCACGTCCTCGAAT
gst-1	CCGTCATCTCGCTCGTCTTAATGG	AGCCTTGCCGTCTTCGTAGTTTC
gst-10	TGGGAAGAGTTCATGGCTTG	AACTTCACTAGAGCCTCCGG
gst-4	AGTTGTTGAACCAGCCCGTGATG	GCCCAAGTCAATGAGTCTCCAACG
prdx-2	TATCGCCTTCTCTGACCGTG	AAGAGTCCACGGAAAGCAATT
sod-1	AAAATGTCGAACCGTGCTGT	CCGGGAGTAAGTCCCTTGAT
sod-2	CTCGCTGCCAGATTTACCAT	TGAACTTGAGAGCTGGCTGA
sod-3	GCAATCTACTGCTCGCACTG	CAGCCTCGTGAAGTTTCTCC
sod-5	AAACGTGCTGTAGCGGTTCT	TCCATGAAGTCCTGGTGACA
trx-1	AGCGGAAGATCTTTGTTCCA	AATTGCGTCTCCATTCTTGG
tba-1	TCATCTCGCAGGTTGTGTCT	GGTAAGCCTTGTCAGCAGAG

666

667 Availability of Data and Materials: *C. elegans* strains JMN080, PHX2923, and PHX2867 are available from
668 the corresponding author upon request. All other strains are available from the *C. elegans* Genome
669 Center. All data and the source video and images are available upon request.

670

671

672 Acknowledgements: This work was funded by NIH awards K99-ES029552 (JHH), NIEHS P42ES010356
673 (JNM), NIEHS T32ES021432 (KSM), and R01ES034270 (JNM), and strains were provided by the
674 Caenorhabditis Genetics Consortium.

675

676 References:

677 1. USDA Sugar Supply: Tables 51-53; US Consumption of Caloric Sweeteners. In: Service USDoAER,
678 editor. 2012.
679 2. Safety WHONaF. Guideline: Sugar Intake for Adults and Children In: Safety NaF, editor.: World
680 Health Organization 2015. p. 49.
681 3. Johnston RD, Stephenson MC, Crossland H, Cordon SM, Palcidi E, Cox EF, et al. No Difference
682 Between High-Fructose and High-Glucose Diets on Liver Triacylglycerol or Biochemistry in Healthy
683 Overweight Men. Gastroenterology. 2013;145(5):1016-25.e2.
684 4. Malik VS, Schulze MB, Hu FB. Intake of sugar-sweetened beverages and weight gain: a
685 systematic review. Am J Clin Nutr. 2006;84(2):274-88.

686 5. Hruby A, Hu FB. The Epidemiology of Obesity: A Big Picture. Pharmacoeconomics.
687 2015;33(7):673-89.
688 6. Health Effects of Overweight and Obesity in 195 Countries over 25 Years. New England Journal
689 of Medicine. 2017;377(1):13-27.
690 7. Palavra NC, Lubomski M, Flood VM, Davis RL, Sue CM. Increased Added Sugar Consumption Is
691 Common in Parkinson's Disease. Front Nutr. 2021;8.
692 8. Haas J, Berg D, Bosy-Westphal A, Schaeffer E. Parkinson’s Disease and Sugar
693 Intake—Reasons for and Consequences of a Still Unclear Craving. Nutrients. 2022;14(15):3240.
694 9. Raza C, Anjum R, Shakeel NuA. Parkinson's disease: Mechanisms, translational models and
695 management strategies. Life Sciences. 2019;226:77-90.
696 10. Santiago JA, Potashkin JA. Blood Biomarkers Associated with Cognitive Decline in Early Stage and
697 Drug-Naive Parkinson’s Disease Patients. PLOS ONE. 2015;10(11):e0142582.
698 11. Mollenhauer B, Zimmermann J, Sixel-Döring F, Focke NK, Wicke T, Ebentheuer J, et al. Baseline
699 predictors for progression 4 years after Parkinson's disease diagnosis in the De Novo Parkinson Cohort
700 (DeNoPa). Mov Disord. 2019;34(1):67-77.
701 12. Palavra NC, Lubomski M, Flood VM, Davis RL, Sue CM. Increased Added Sugar Consumption Is
702 Common in Parkinson's Disease. Front Nutr. 2021;8:628845-.
703 13. Sánchez-Gómez A, Alcarraz-Vizán G, Fernández M, Fernández-Santiago R, Ezquerra M, Cámara
704 A, et al. Peripheral insulin and amylin levels in Parkinson's disease. Parkinsonism & Related Disorders.
705 2020;79:91-6.
706 14. Mondoux MA, Love DC, Ghosh SK, Fukushige T, Bond M, Weerasinghe GR, et al. O-Linked-N-
707 Acetylglucosamine Cycling and Insulin Signaling Are Required for the Glucose Stress Response in
708 Caenorhabditis elegans. Genetics. 2011;188(2):369-82.
709 15. Alcántar-Fernández J, Navarro RE, Salazar-Martínez AM, Pérez-Andrade ME, Miranda-Ríos J.
710 Caenorhabditis elegans respond to high-glucose diets through a network of stress-responsive
711 transcription factors. PLOS ONE. 2018;13(7):e0199888.
712 16. Alcántar-Fernández J, González-Maciel A, Reynoso-Robles R, Pérez Andrade ME, Hernández-
713 Vázquez AdJ, Velázquez-Arellano A, et al. High-glucose diets induce mitochondrial dysfunction in
714 Caenorhabditis elegans. PLOS ONE. 2019;14(12):e0226652.
715 17. Salim C, Rajini PS. Glucose feeding during development aggravates the toxicity of the
716 organophosphorus insecticide Monocrotophos in the nematode, Caenorhabditis elegans. Physiology &
717 Behavior. 2014;131:142-8.
718 18. Salim C, Rajini PS. Glucose-rich diet aggravates monocrotophos-induced dopaminergic neuronal
719 dysfunction in Caenorhabditis elegans. Journal of Applied Toxicology. 2017;37(6):772-80.
720 19. Garcia AM, Ladage ML, Dumesnil DR, Zaman K, Shulaev V, Azad RK, et al. Glucose Induces
721 Sensitivity to Oxygen Deprivation and Modulates Insulin/IGF-1 Signaling and Lipid Biosynthesis in
722 Caenorhabditis elegans. Genetics. 2015;200(1):167-84.
723 20. Lodha D, Rajasekaran S, Jayavelu T, Subramaniam JR. Detrimental effects of fructose on
724 mitochondria in mouse motor neurons and on C. elegans healthspan. Nutritional Neuroscience. 2020:1-
725 10.
726 21. Cooper JF, Van Raamsdonk JM. Modeling Parkinson's Disease in C. elegans. J Parkinsons Dis.
727 2018;8(1):17-32.
728 22. Caldwell KA, Willicott CW, Caldwell GA. Modeling neurodegeneration in Caenorhabditiselegans.
729 Dis Model Mech. 2020;13(10).
730 23. Pinkas A, Lawes M, Aschner M. System-specific neurodegeneration following glucotoxicity in the
731 C. elegans model. NeuroToxicology. 2018;68:88-90.
732 24. Li Y, Chen Q, Liu Y, Bi L, Jin L, Xu K, et al. High glucose-induced ROS-accumulation in embryo-
733 larval stages of zebrafish leads to mitochondria-mediated apoptosis. Apoptosis. 2022;27(7):509-20.

25. Barouki R, Gluckman PD, Grandjean P, Hanson M, Heindel JJ. Developmental origins of non-communicable disease: Implications for research and public health. Environmental Health. 2012;11(1):42.
26. Grandjean P, Barouki R, Bellinger DC, Casteleyn L, Chadwick LH, Cordier S, et al. Life-Long Implications of Developmental Exposure to Environmental Stressors: New Perspectives. Endocrinology. 2015;156(10):3408-15.
27. Hershberger KA, Rooney JP, Turner EA, Donoghue LJ, Bodhicharla R, Maurer LL, et al. Early-life mitochondrial DNA damage results in lifelong deficits in energy production mediated by redox signaling in Caenorhabditis elegans. Redox Biology. 2021;43:102000.
28. Mello DF, Bergemann CM, Fisher K, Chitrakar R, Bijwadia SR, Wang Y, et al. Rotenone Modulates Caenorhabditis elegans Immunometabolism and Pathogen Susceptibility. Front Immunol. 2022;13:840272.
29. Schober A. Classic toxin-induced animal models of Parkinson's disease: 6-OHDA and MPTP. Cell and Tissue Research. 2004;318(1):215-24.
30. Bijwadia SR, Morton KS, Meyer JN. Quantifying Levels of Dopaminergic Neuron Morphological Alteration and Degeneration in Caenorhabditis elegans. JoVE.e62894.
31. Masoudi N, Ibanez-Cruceyra P, Offenburger S-L, Holmes A, Gartner A. Tetraspanin (TSP-17) Protects Dopaminergic Neurons against 6-OHDA-Induced Neurodegeneration in C. elegans. PLOS Genetics. 2014;10(12):e1004767.
32. Nass R, Hall DH, Miller DM, Blakely RD. Neurotoxin-induced degeneration of dopamine neurons in Caenorhabditis elegans. Proceedings of the National Academy of Sciences. 2002;99(5):3264-9.
33. Yu T, Robotham JL, Yoon Y. Increased production of reactive oxygen species in hyperglycemic conditions requires dynamic change of mitochondrial morphology. Proceedings of the National Academy of Sciences. 2006;103(8):2653-8.
34. Youle RJ, van der Bliek AM. Mitochondrial Fission, Fusion, and Stress. Science. 2012;337(6098):1062-5.
35. Meyer JN, Leuthner TC, Luz AL. Mitochondrial fusion, fission, and mitochondrial toxicity. Toxicology. 2017;391:42-53.
36. Yu T, Sheu S-S, Robotham JL, Yoon Y. Mitochondrial fission mediates high glucose-induced cell death through elevated production of reactive oxygen species. Cardiovascular Research. 2008;79(2):341-51.
37. Jadiya P, Garbincius JF, Elrod JW. Reappraisal of metabolic dysfunction in neurodegeneration: Focus on mitochondrial function and calcium signaling. Acta Neuropathologica Communications. 2021;9(1):124.
38. Pathak D, Shields LY, Mendelsohn BA, Haddad D, Lin W, Gerencser AA, et al. The Role of Mitochondrially Derived ATP in Synaptic Vesicle Recycling Journal of Biological Chemistry. 2015;290(37):22325-36.
39. Gusarov I, Pani B, Gautier L, Smolentseva O, Eremina S, Shamovsky I, et al. Glycogen controls Caenorhabditis elegans lifespan and resistance to oxidative stress. Nat Commun. 2017;8:15868.
40. Duerr JS, Frisby DL, Gaskin J, Duke A, Asermely K, Huddleston D, et al. The cat-1 Gene of Caenorhabditis elegansEncodes a Vesicular Monoamine Transporter Required for Specific Monoamine-Dependent Behaviors. The Journal of Neuroscience. 1999;19(1):72-84.
41. Schlotterer A, Kukudov G, Bozorgmehr F, Hutter H, Du X, Oikonomou D, et al. C. elegans as Model for the Study of High Glucose– Mediated Life Span Reduction. Diabetes. 2009;58(11):2450-6.
42. Tauffenberger A, Parker JA. Heritable Transmission of Stress Resistance by High Dietary Glucose in Caenorhabditis elegans. PLOS Genetics. 2014;10(5):e1004346.
43. Zhu G, Yin F, Wang L, Wei W, Jiang L, Qin J. Modeling type 2 diabetes-like hyperglycemia in C. elegans on a microdevice. Integr Biol (Camb). 2016;8(1):30-8.

782 44. Lee S-J, Murphy CT, Kenyon C. Glucose Shortens the Life Span of C. elegans by Downregulating
783 DAF-16/FOXO Activity and Aquaporin Gene Expression. Cell Metabolism. 2009;10(5):379-91.
784 45. Liggett MR, Hoy MJ, Mastroianni M, Mondoux MA. High-glucose diets have sex-specific effects
785 on aging in C. elegans: toxic to hermaphrodites but beneficial to males. Aging (Albany NY).
786 2015;7(6):383-8.
787 46. Teshiba E, Miyahara K, Takeya H. Glucose-induced abnormal egg-laying rate in Caenorhabditis
788 elegans. Bioscience, Biotechnology, and Biochemistry. 2016;80(7):1436-9.
789 47. Zheng J, Gao C, Wang M, Tran P, Mai N, Finley JW, et al. Lower Doses of Fructose Extend
790 Lifespan in Caenorhabditis elegans. Journal of Dietary Supplements. 2017;14(3):264-77.
791 48. Ke W, Reed JN, Yang C, Higgason N, Rayyan L, Wählby C, et al. Genes in human obesity loci are
792 causal obesity genes in C. elegans. PLOS Genetics. 2021;17(9):e1009736.
793 49. Gatrell L, Wilkins W, Rana P, Farris M. Glucose effects on polyglutamine-induced proteotoxic
794 stress in Caenorhabditis elegans. Biochemical and Biophysical Research Communications.
795 2020;522(3):709-15.
796 50. Beaudoin-Chabot C, Wang L, Celik C, Abdul Khalid AT-F, Thalappilly S, Xu S, et al. The unfolded
797 protein response reverses the effects of glucose on lifespan in chemically-sterilized C. elegans. Nature
798 Communications. 2022;13(1):5889.
799 51. Engstrom AK, Davis CD, Erichsen JL, Mondoux MA. Timing of High-glucose Diet in the C. elegans
800 Lifecycle Impacts Fertility Phenotypes. MicroPubl Biol. 2022;2022.
801 52. Mondoux MA, Love DC, Ghosh SK, Fukushige T, Bond M, Weerasinghe GR, et al. O-linked-N-
802 acetylglucosamine cycling and insulin signaling are required for the glucose stress response in
803 Caenorhabditis elegans. Genetics. 2011;188(2):369-82.
804 53. Wang X, Zhang L, Zhang L, Wang W, Wei S, Wang J, et al. Effects of excess sugars and lipids on
805 the growth and development of Caenorhabditis elegans. Genes & Nutrition. 2020;15(1):1.
806 54. Russell JW, Golovoy D, Vincent AM, Mahendru P, Olzmann JA, Mentzer A, et al. High glucose-
807 induced oxidative stress and mitochondrial dysfunction in neurons. The FASEB Journal.
808 2002;16(13):1738-48.
809 55. de Guzman ACV, Kang S, Kim EJ, Kim JH, Jang N, Cho JH, et al. High-Glucose Diet Attenuates the
810 Dopaminergic Neuronal Function in C. elegans, Leading to the Acceleration of the Aging Process. ACS
811 Omega. 2022;7(36):32339-48.
812 56. Gonzalez-Hunt CP, Luz AL, Ryde IT, Turner EA, Ilkayeva OR, Bhatt DP, et al. Multiple metabolic
813 changes mediate the response of Caenorhabditis elegans to the complex I inhibitor rotenone.
814 Toxicology. 2021;447:152630.
815 57. Sherer TB, Betarbet R, Testa CM, Seo BB, Richardson JR, Kim JH, et al. Mechanism of toxicity in
816 rotenone models of Parkinson's disease. J Neurosci. 2003;23(34):10756-64.
817 58. Sherer TB, Richardson JR, Testa CM, Seo BB, Panov AV, Yagi T, et al. Mechanism of toxicity of
818 pesticides acting at complex I: relevance to environmental etiologies of Parkinson's disease. J
819 Neurochem. 2007;100(6):1469-79.
820 59. McDonald PW, Hardie SL, Jessen TN, Carvelli L, Matthies DS, Blakely RD. Vigorous motor activity
821 in Caenorhabditis elegans requires efficient clearance of dopamine mediated by synaptic localization of
822 the dopamine transporter DAT-1. J Neurosci. 2007;27(51):14216-27.
823 60. Gabriel LR, Wu S, Kearney P, Bellvé KD, Standley C, Fogarty KE, et al. Dopamine Transporter
824 Endocytic Trafficking in Striatal Dopaminergic Neurons: Differential Dependence on Dynamin and the
825 Actin Cytoskeleton. The Journal of Neuroscience. 2013;33(45):17836-46.
826 61. Loder MK, Melikian HE. The dopamine transporter constitutively internalizes and recycles in a
827 protein kinase C-regulated manner in stably transfected PC12 cell lines. J Biol Chem.
828 2003;278(24):22168-74.

829 62. Geraldes P, King GL. Activation of protein kinase C isoforms and its impact on diabetic
830 complications. Circ Res. 2010;106(8):1319-31.
831 63. Campbell E, Schlappal A, Geller E, Castonguay TW. Chapter 19 - Fructose-Induced
832 Hypertriglyceridemia: A Review. In: Watson RR, editor. Nutrition in the Prevention and Treatment of
833 Abdominal Obesity. San Diego: Academic Press; 2014. p. 197-205.
834 64. Singh AR, Joshi S, Arya R, Kayastha AM, Srivastava KK, Tripathi LM, et al. Molecular cloning and
835 characterization of Brugia malayi hexokinase. Parasitology International. 2008;57(3):354-61.
836 65. Softic S, Meyer JG, Wang G-X, Gupta MK, Batista TM, Lauritzen HPMM, et al. Dietary Sugars
837 Alter Hepatic Fatty Acid Oxidation via Transcriptional and Post-translational Modifications of
838 Mitochondrial Proteins. Cell Metabolism. 2019;30(4):735-53.e4.
839 66. Su LJ, Mahabir S, Ellison G, McGuinn L, Reid B. Epigenetic Contributions to the Relationship
840 between Cancer and Dietary Intake of Nutrients, Bioactive Food Components, and Environmental
841 Toxicants. Frontiers in Genetics. 2012;2.
842 67. Mattsson JL. Mixtures in the real world: The importance of plant self-defense toxicants,
843 mycotoxins, and the human diet. Toxicology and Applied Pharmacology. 2007;223(2):125-32.
844 68. Mahaffey KR, Vanderveen JE. Nutrient-toxicant interactions: susceptible populations.
845 Environmental Health Perspectives. 1979;29:81-7.
846 69. Odland J, Deutch B, Hansen J, Burkow I. The importance of diet on exposure to and effects of
847 persistent organic pollutants on human health in the Arctic. Acta Paediatrica. 2003;92(11):1255-66.
848 70. Den Broeder MJ, Moester MJB, Kamstra JH, Cenijn PH, Davidoiu V, Kamminga LM, et al. Altered
849 Adipogenesis in Zebrafish Larvae Following High Fat Diet and Chemical Exposure Is Visualised by
850 Stimulated Raman Scattering Microscopy. International Journal of Molecular Sciences. 2017;18(4):894.
851 71. Branco AT, Lemos B. High Intake of Dietary Sugar Enhances Bisphenol A (BPA) Disruption and
852 Reveals Ribosome-Mediated Pathways of Toxicity. Genetics. 2014;197(1):147-57.
853 72. Liu J, Gupta RC, Goad JT, Karanth S, Pope C. Modulation of parathion toxicity by glucose feeding:
854 Is nitric oxide involved? Toxicology and Applied Pharmacology. 2007;219(2):106-13.
855 73. Sherwood DR, Butler JA, Kramer JM, Sternberg PW. FOS-1 promotes basement-membrane
856 removal during anchor-cell invasion in C. elegans. Cell. 2005;121(6):951-62.
857 74. Redemann S, Schloissnig S, Ernst S, Pozniakowsky A, Ayloo S, Hyman AA, et al. Codon
858 adaptation-based control of protein expression in C. elegans. Nat Methods. 2011;8(3):250-2.
859 75. Cothren SD, Meyer JN, Hartman JH. Blinded Visual Scoring of Images Using the Freely-available
860 Software Blinder. Bio Protoc. 2018;8(23).
861 76. Luz AL, Smith LL, Rooney JP, Meyer JN. Seahorse Xfe 24 Extracellular Flux Analyzer-Based
862 Analysis of Cellular Respiration in Caenorhabditis elegans. Curr Protoc Toxicol. 2015;66:25.7.1-.7.15.
863 77. Luz AL, Lagido C, Hirschey MD, Meyer JN. In Vivo Determination of Mitochondrial Function Using
864 Luciferase-Expressing Caenorhabditis elegans: Contribution of Oxidative Phosphorylation, Glycolysis, and
865 Fatty Acid Oxidation to Toxicant-Induced Dysfunction. Curr Protoc Toxicol. 2016;69:25.8.1-.8.2.

866

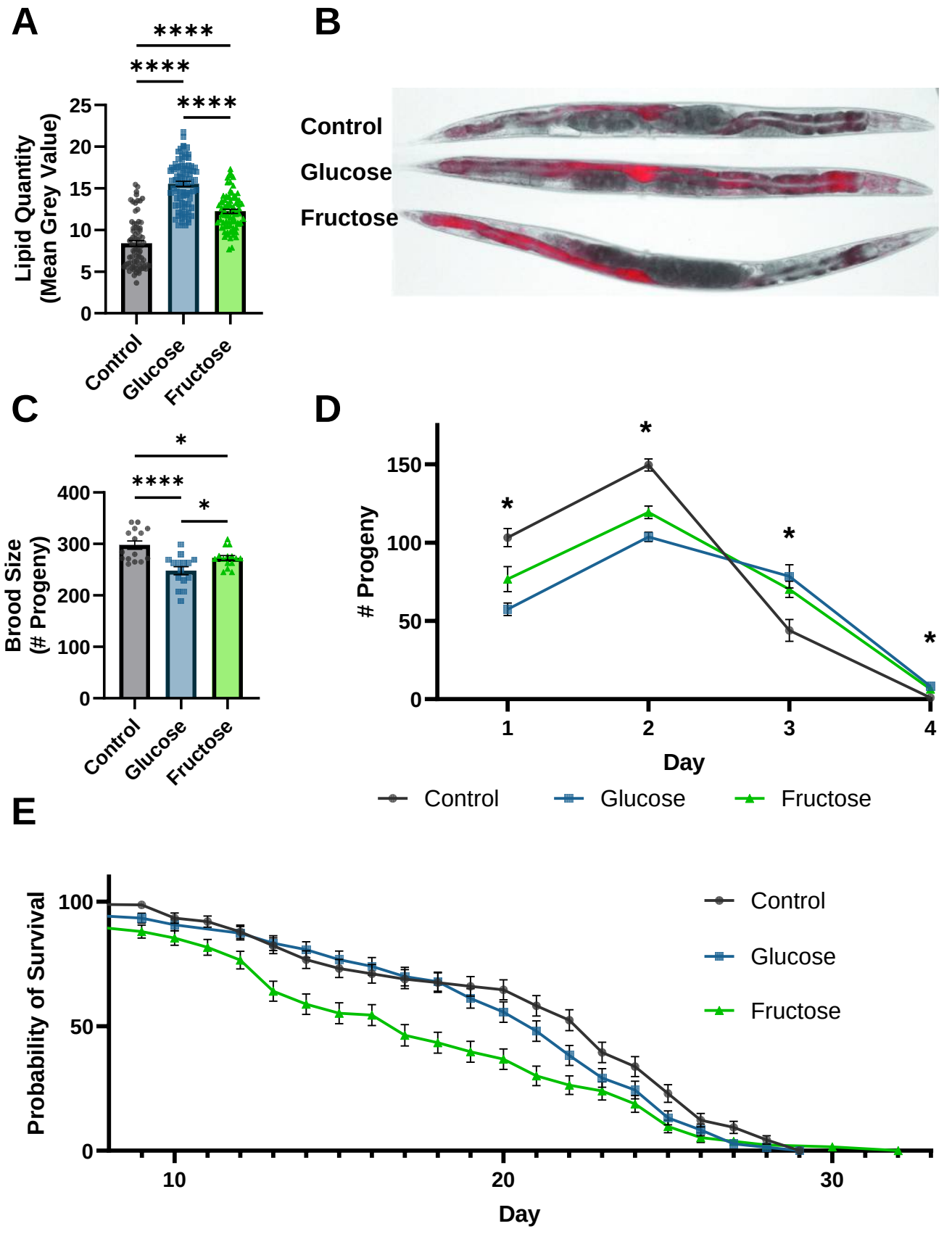
A
****
****
****
Lipid Quantity
(Mean Grey Value)
25
20
15
10
5
0
Control
Glucose
Fructose
B
Control
Glucose
Fructose
C
*
****
*
Brood Size
(# Progeny)
400
300
200
100
0
Control
Glucose
Fructose
D
*
*
*
*
Progeny
150
100
50
0
1
2
3
4
Day
Control
Glucose
Fructose
E
Probability of Survival
100
50
0
10
20
30
Day
Control
Glucose
Fructose

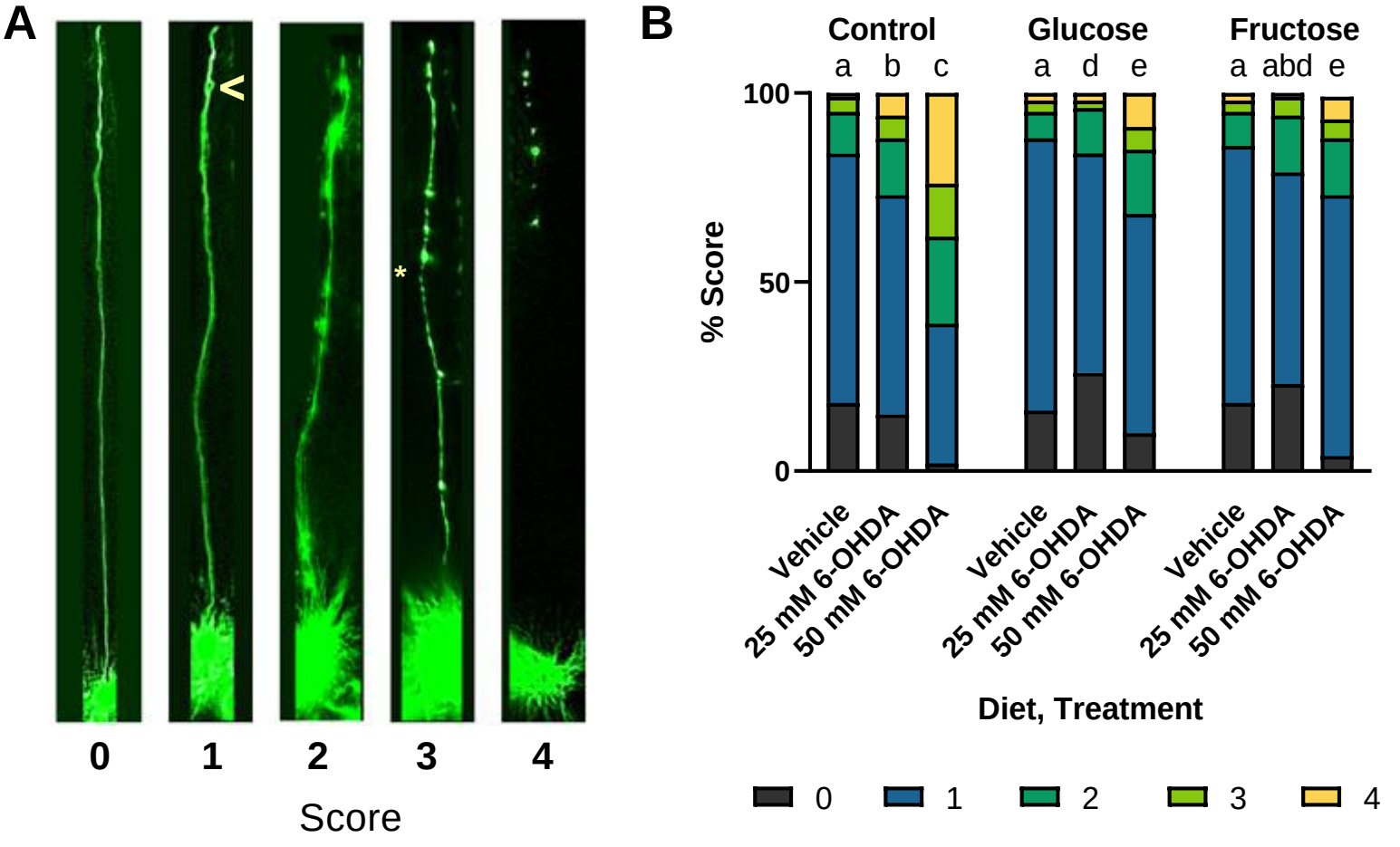
A
<
*
0
1
2
3
4
Score
B
Control
Glucose
Fructose
a b c
a d e
a abd e
100
50
0
% Score
Vehicle
25 mM 6-OHDA
50 mM 6-OHDA
Vehicle
25 mM 6-OHDA
50 mM 6-OHDA
Vehicle
25 mM 6-OHDA
50 mM 6-OHDA
Diet, Treatment
0
1
2
3
4

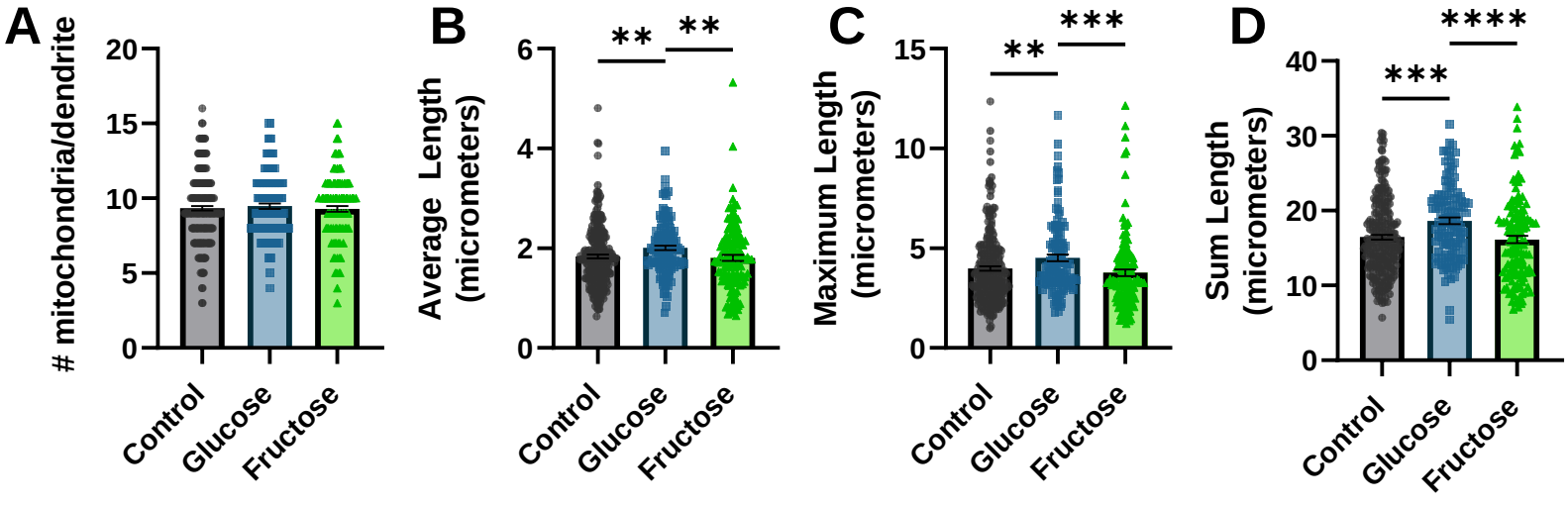
A
mitochondria/dendrite
20
15
10
5
0
Control
Glucose
Fructose
B
Average Length (micrometers)
6
4
2
0
**
**
Control
Glucose
Fructose
C
Maximum Length (micrometers)
15
10
5
0
**
***
Control
Glucose
Fructose
D
Sum Length (micrometers)
40
30
20
10
0
***
****
Control
Glucose
Fructose

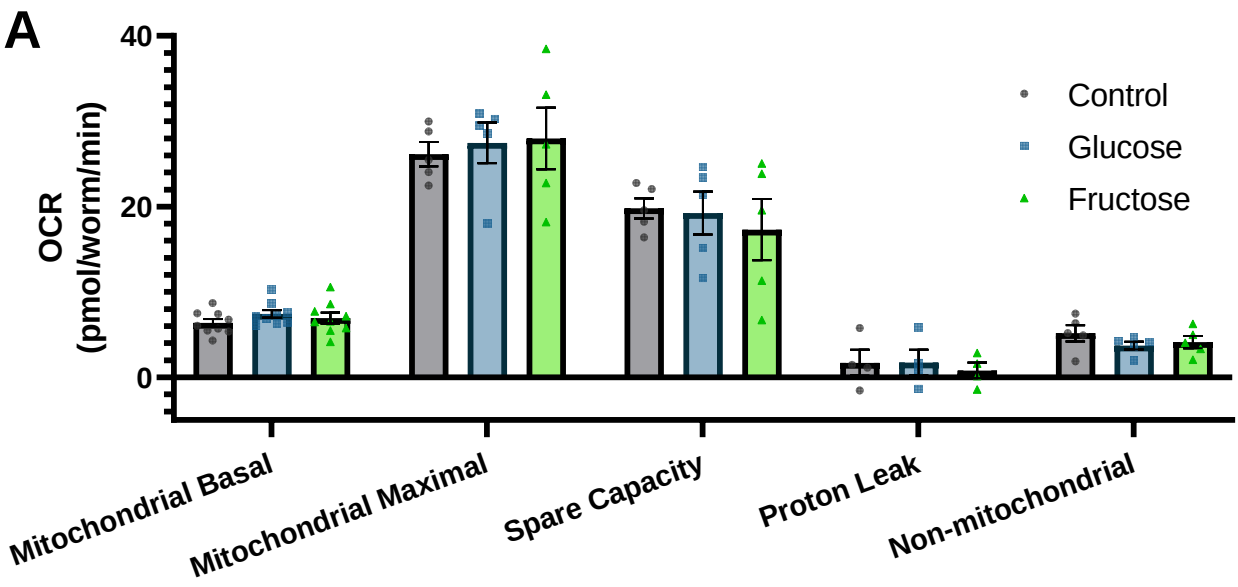
A
OCR
(pmol/worm/min)
40
20
0
Control
Glucose
Fructose
Mitochondrial Basal
Mitochondrial Maximal
Spare Capacity
Proton Leak
Non-mitochondrial

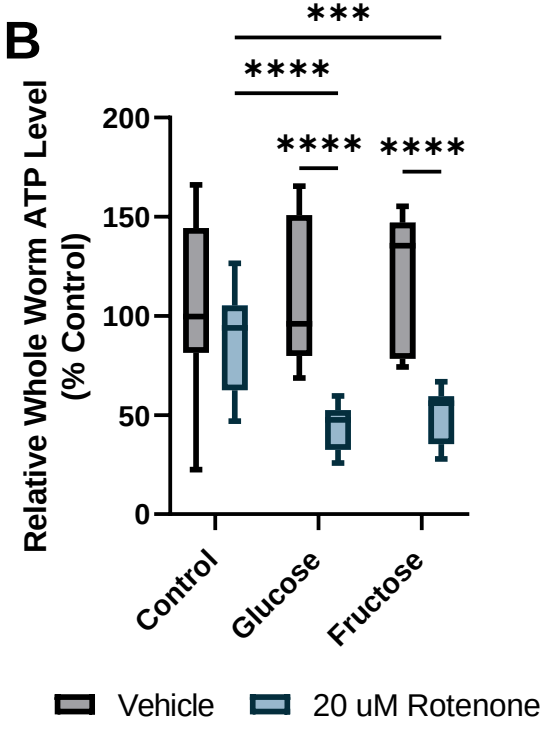
B
Relative Whole Worm ATP Level
(% Control)
200
150
100
50
0
***
****
****
****
Control
Glucose
Fructose
Vehicle
20 uM Rotenone

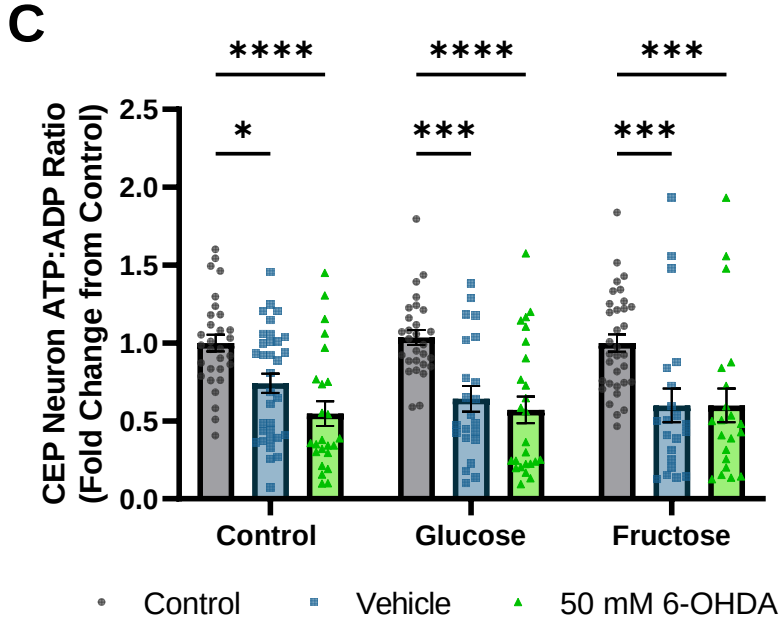
C
CEP Neuron ATP:ADP Ratio
(Fold Change from Control)
2.5
2.0
1.5
1.0
0.5
0.0
****
****
***
*
***
***
Control
Glucose
Fructose
Control
Vehicle
50 mM 6-OHDA

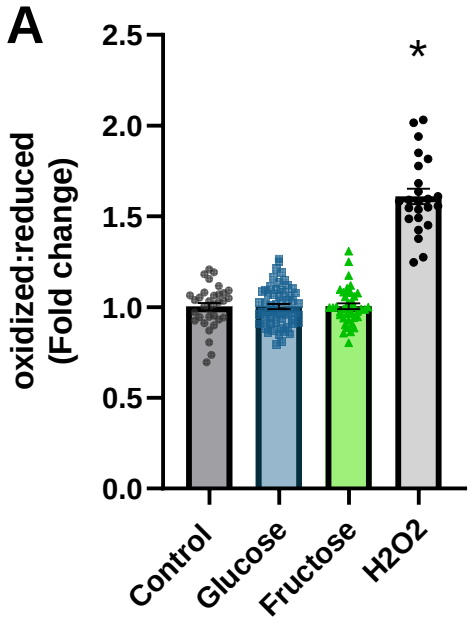
A
oxidized:reduced
(Fold change)
2.5
2.0
1.5
1.0
0.5
0.0
*
Control
Glucose
Fructose
H2O2

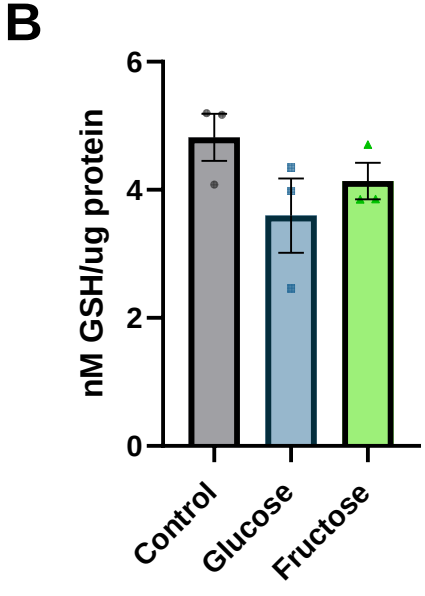
B
nM GSH/ug protein
6
4
2
0
Control
Glucose
Fructose

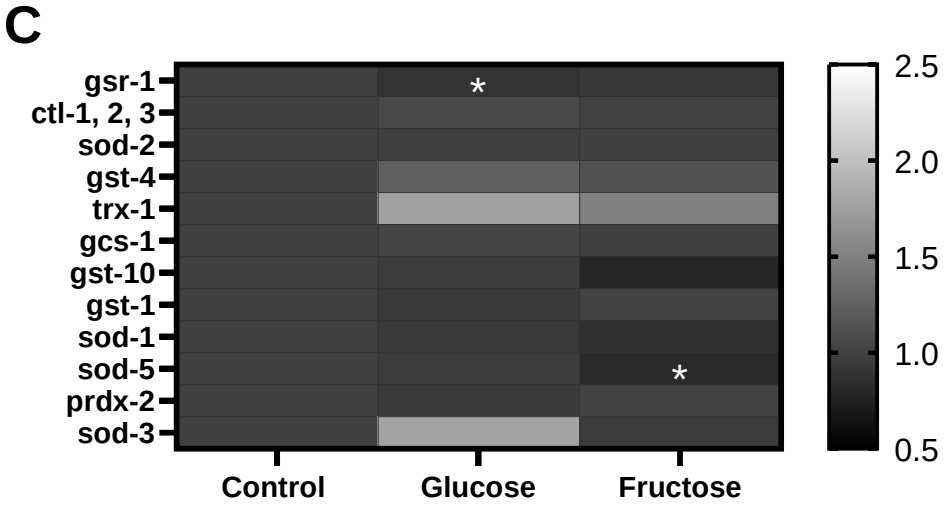
C
gsr-1
ctl-1, 2, 3
sod-2
gst-4
trx-1
gcs-1
gst-10
gst-1
sod-1
sod-5
prdx-2
sod-3
*
*
Control
Glucose
Fructose
2.5
2.0
1.5
1.0
0.5

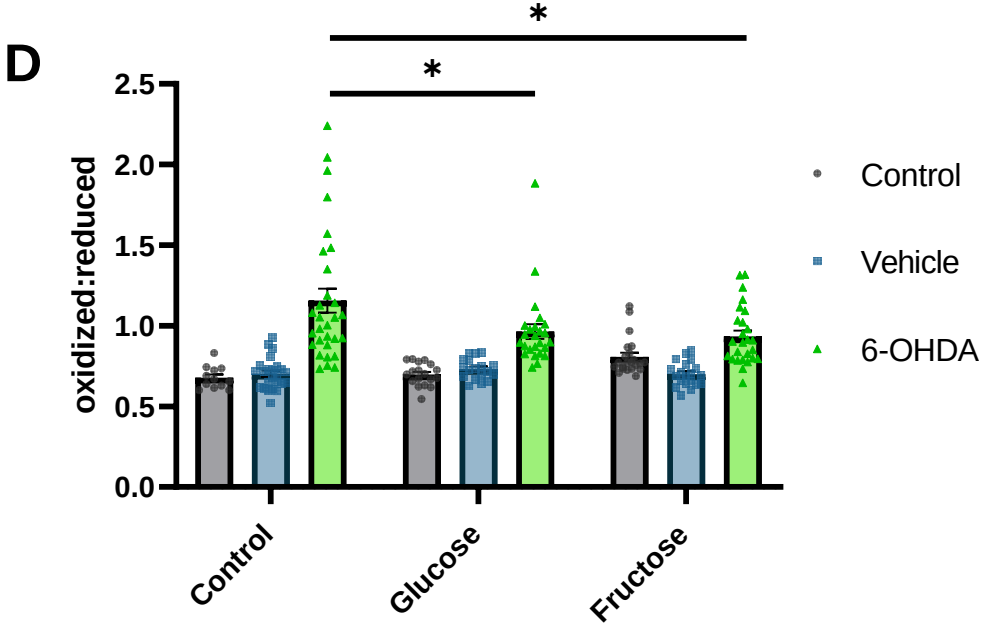
D
oxidized:reduced
2.5
2.0
1.5
1.0
0.5
0.0
*
*
Control
Glucose
Fructose
Control
Vehicle
6-OHDA

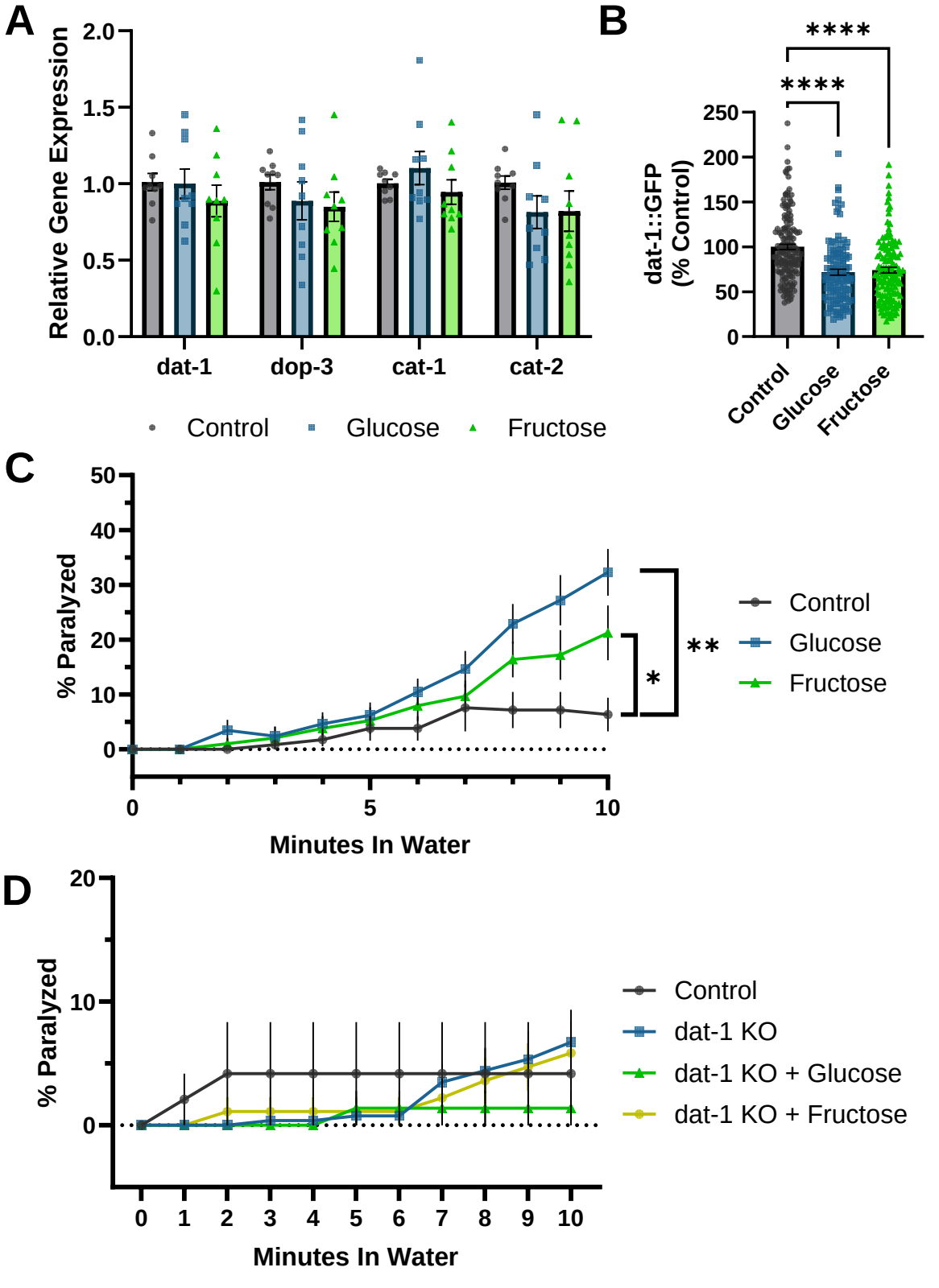
A
Relative Gene Expression
2.0
1.5
1.0
0.5
0.0
dat-1
dop-3
cat-1
cat-2
Control
Glucose
Fructose
B
****
****
dat-1::GFP
(% Control)
250
200
150
100
50
0
Control
Glucose
Fructose
C
% Paralyzed
50
40
30
20
10
0
0
5
10
Minutes In Water
**
*
Control
Glucose
Fructose
D
% Paralyzed
20
10
0
0
1
2
3
4
5
6
7
8
9
10
Minutes In Water
Control
dat-1 KO
dat-1 KO + Glucose
dat-1 KO + Fructose